Exploring blazar jets with multi-wavelength and multi-timescale variability studies

Gopal Bhatta
Nuclear Institute of Physics PAN
Krakow, Poland

Nuclear Institute of Physics PAN
Krakow, Poland
2021/03/09

Outline

- Active Galactic Nuclei
- Blazars Jets
- Variability – Microvariability, long-term variabiliy
- Radio, Optical, X-ray and gamma-ray variability
- Quasi-periodic oscillations
- Possible interpretations
- Summary

Active Galactic Nuclei Observed Properties

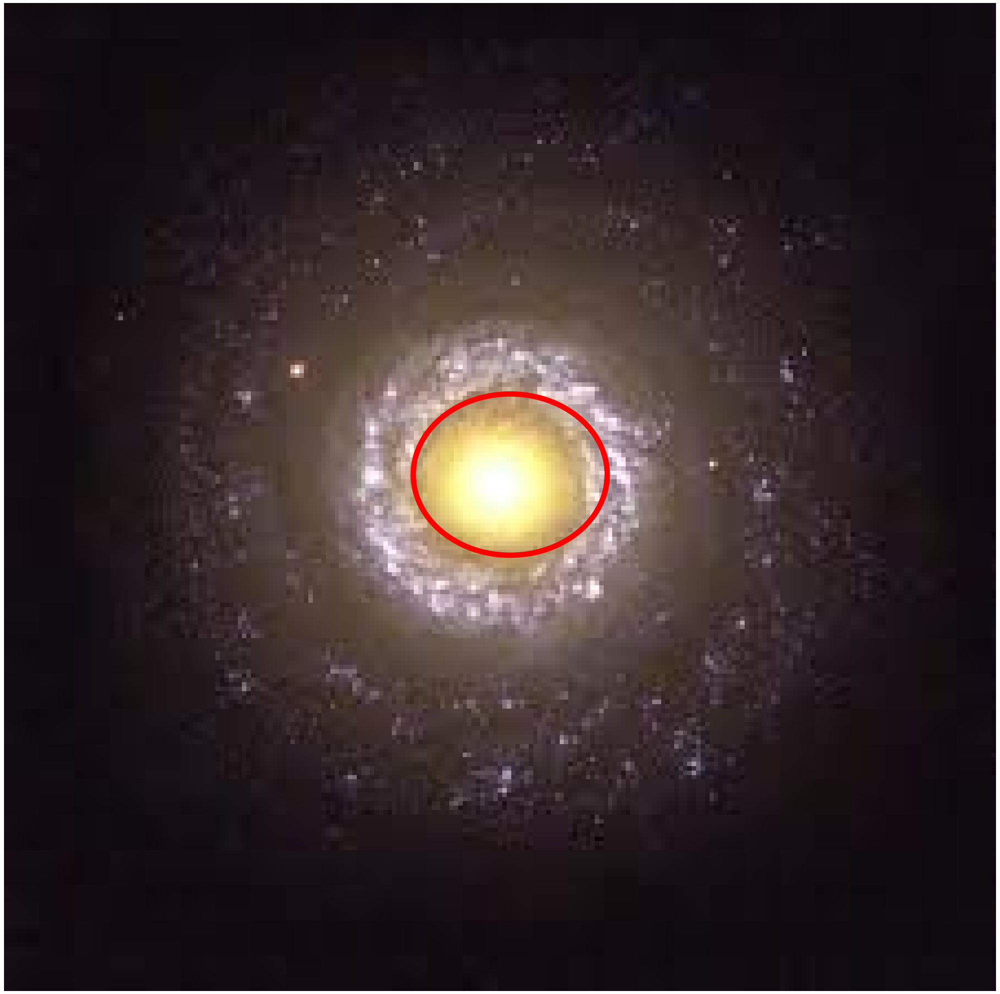

- Active galactic core (~ 1-10 % central region) of distant (high redshift up to 6.4) galaxy
- High Luminosity (~ 10^{-2} - 10^{4} a typical galaxy)
- Multi-frequency variability in all frequency ranges and over all timescales.
- Non-thermal emission
- Broad emission lines
- Narrow emission lines

AGN - Physical Properties

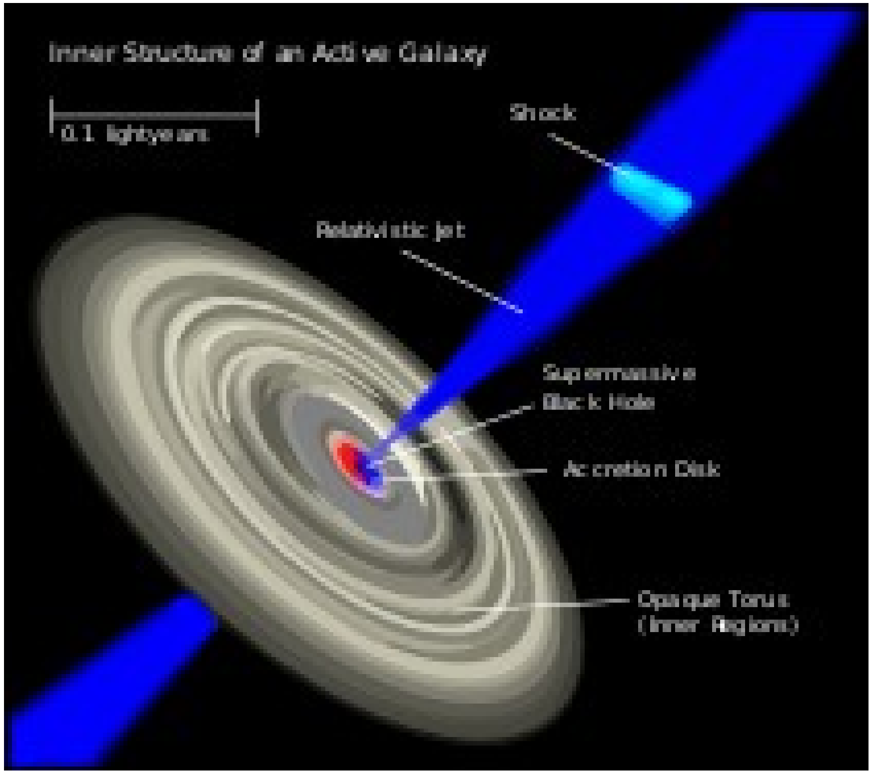

- Supermassive black hole $\sim 10^9$M
- Accretion disk ~ 0.1-1.0 pc
- Relativistic jets ~kpc

AGN Standard Model Classification

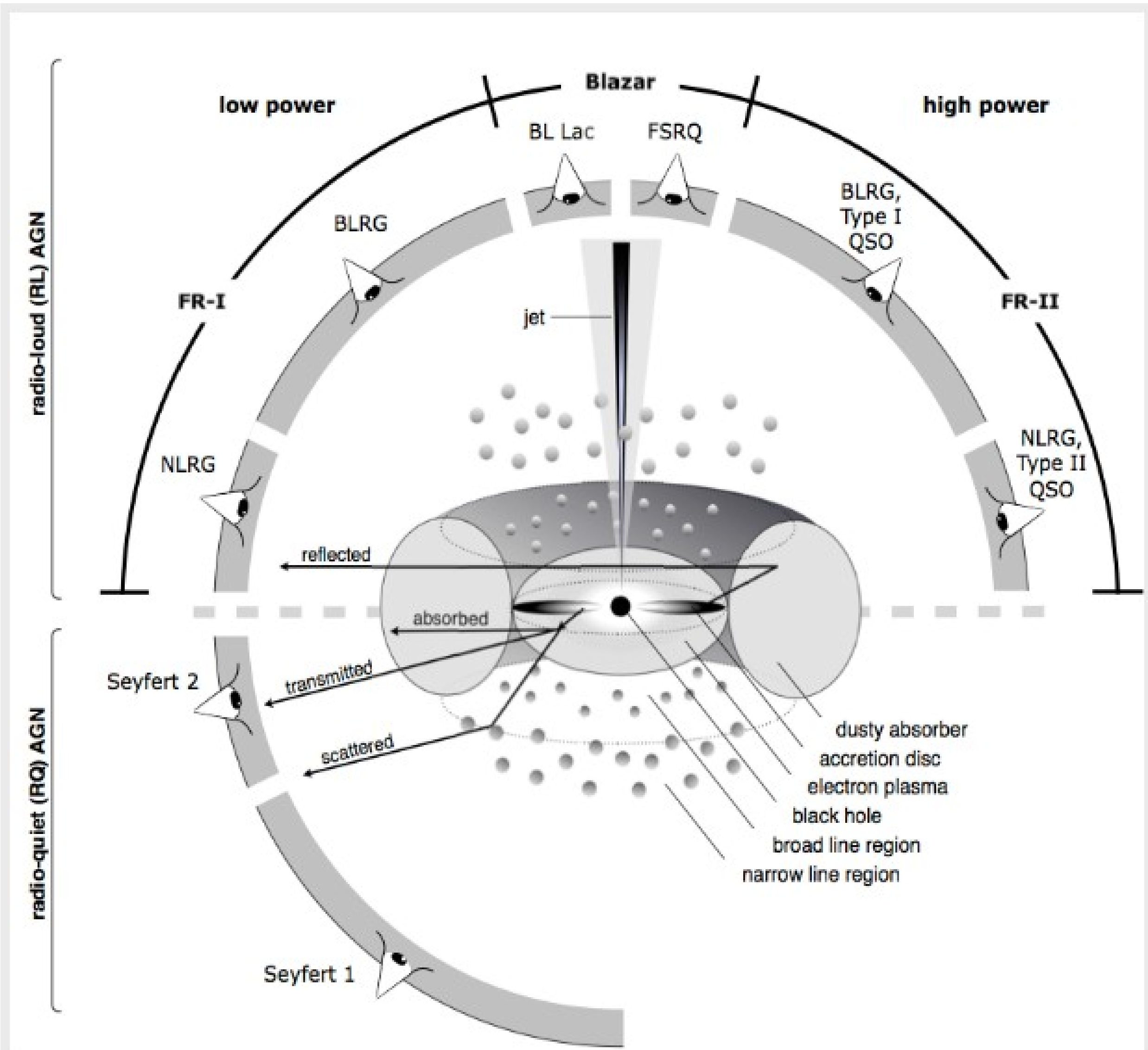

Sketch of the basic ideas of the unified AGN model. Credit: Beckmann & Shrader (2012).

- Unified AGN model classification is based on the jet angle with the line of sight. In this model, AGN phenomenology mainly results due to jet orientation.

AGN Jets

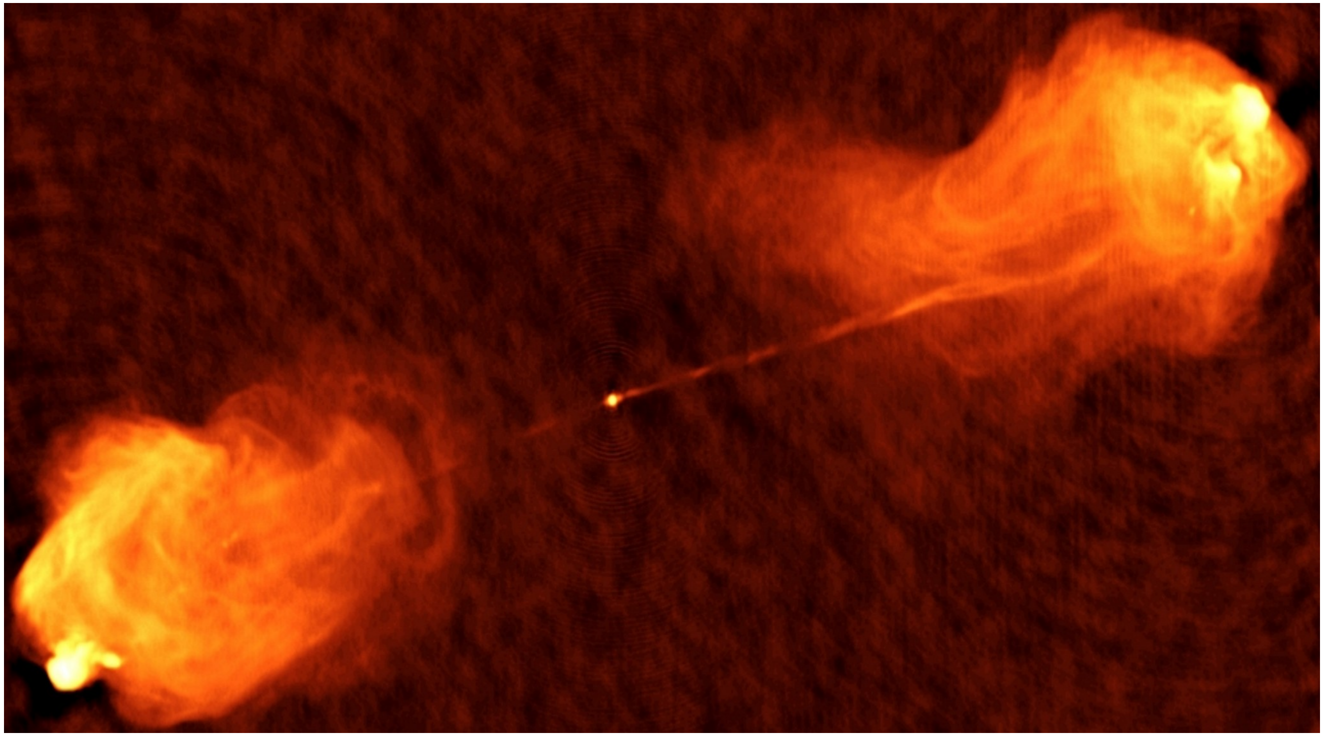

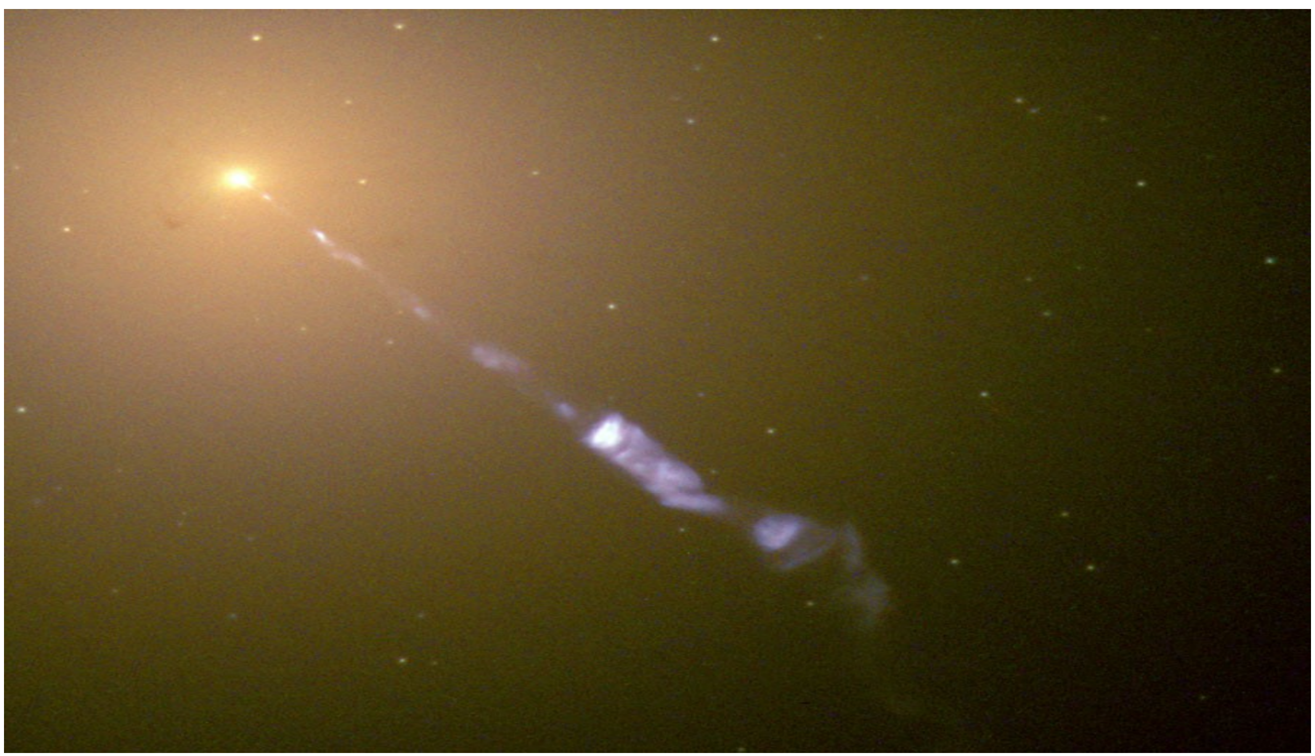

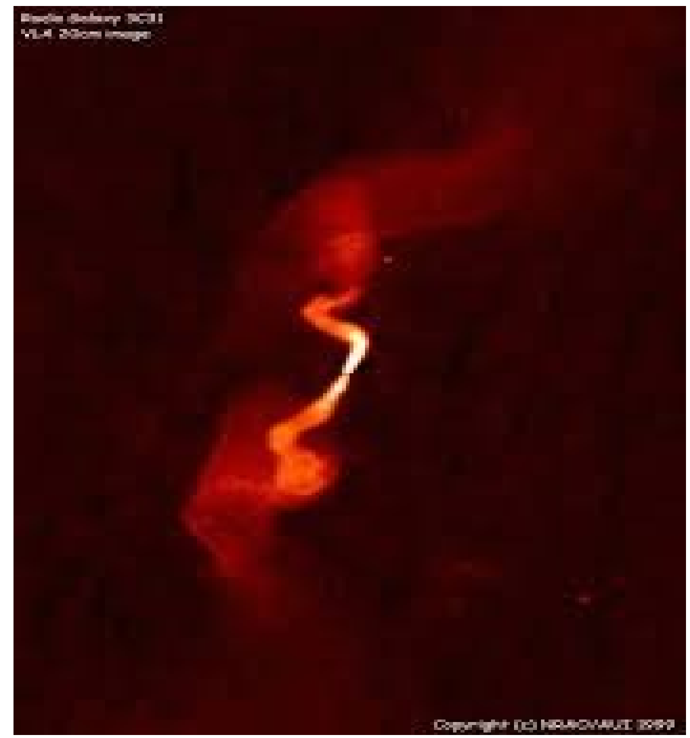

Cygnus A, M87 and 3C31

What are Blazars?

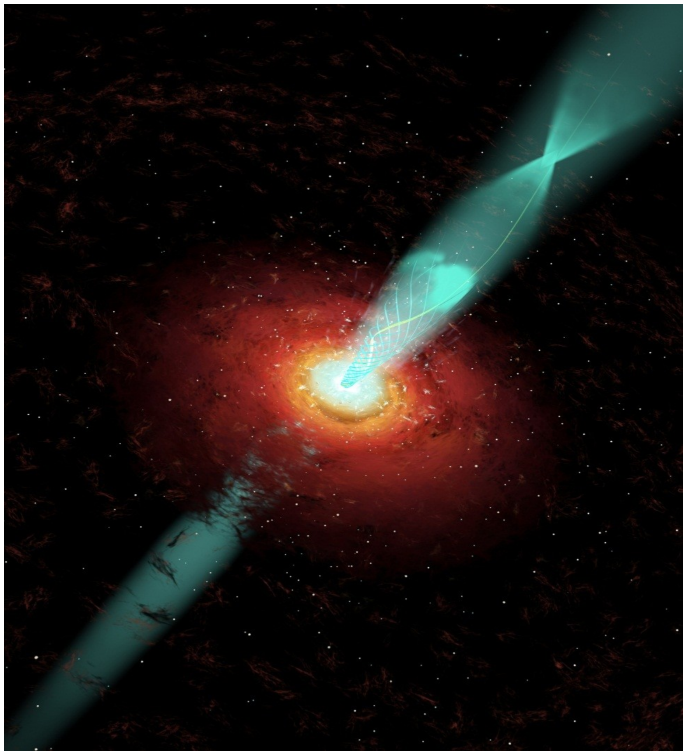

- Characterized by high amplitude rapid variability, high optical and radio polarization, non-thermal multi-frequency (from radio to gamma-ray) variable flux

Doppler Factor

$$\delta=\gamma^{-1}\left(1-\beta\cos\theta\right)^{-1} \text{ where } \beta=v/c\text{, frequency } \nu=\delta\nu'$$

- **Blazars are a subset of active galactic nuclei (AGN), with relativistic jets oriented at small angles to the line of sight of the observer.**

$\theta \sim 5^{\circ}$

blazar

Blazar SED and Blazar sequence

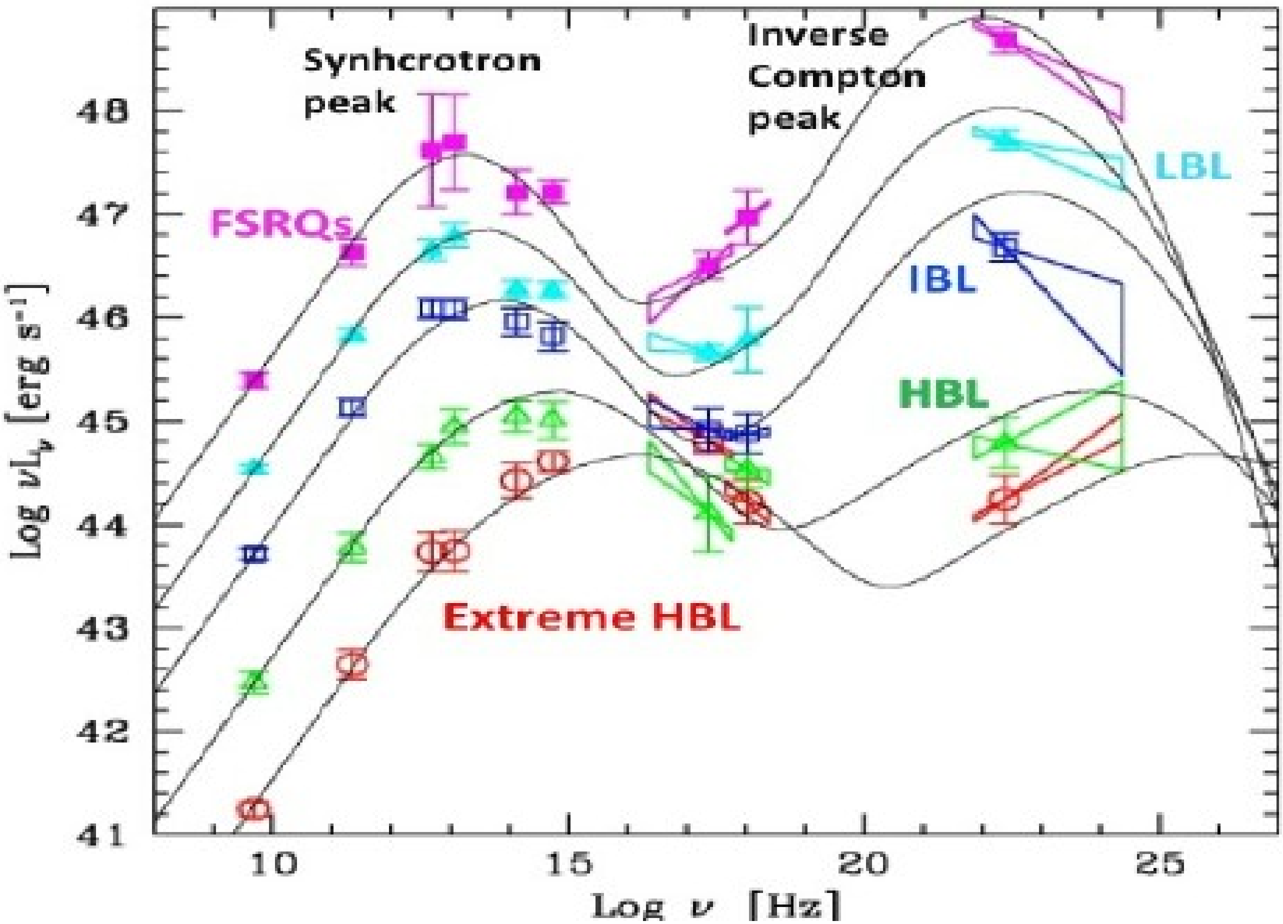

Types of Variability in Blazars

Type	Flux Variability	Time Scale	Apparent Source
Long Term	~ 5 Magnitudes	Years	Change in Accretion Rate
Short Term (Flare)	~ Few Magnitudes	Weeks to months	Passage of shock wave along the Jet
Microvariability (Intraday)	Up to 1 Magnitude	Minutes to a day	Inhomogeneity in the plasma material in the Jet

Poon et al. 2009

Microvariability

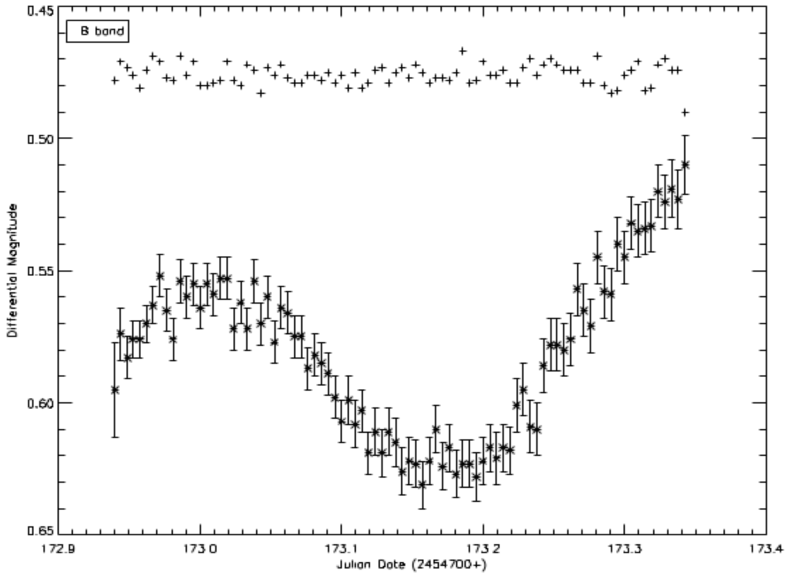

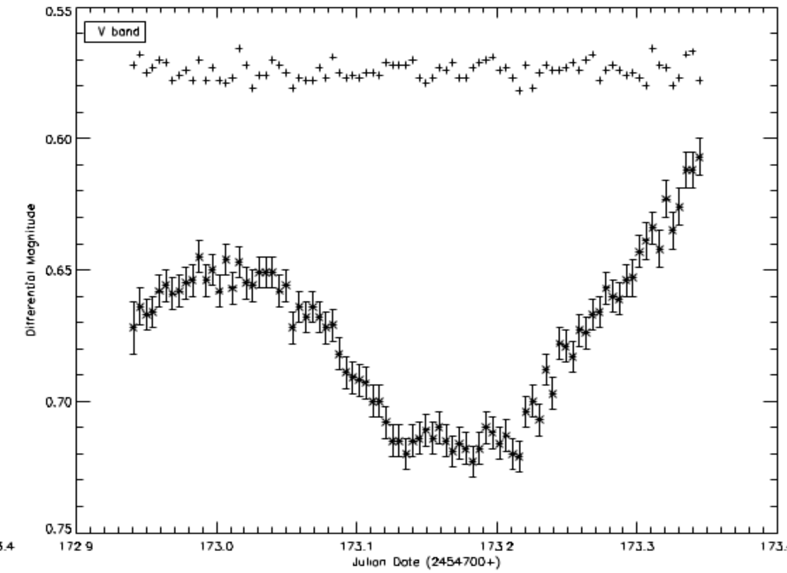

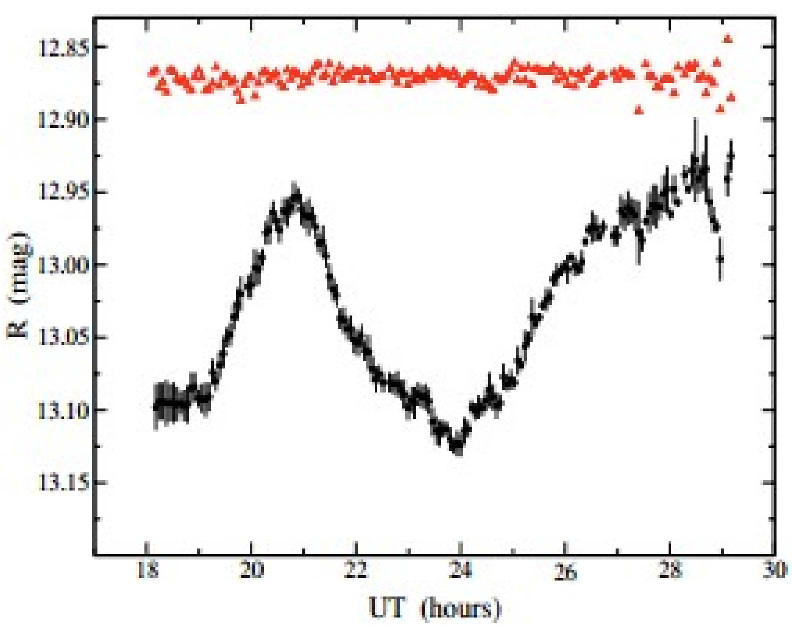

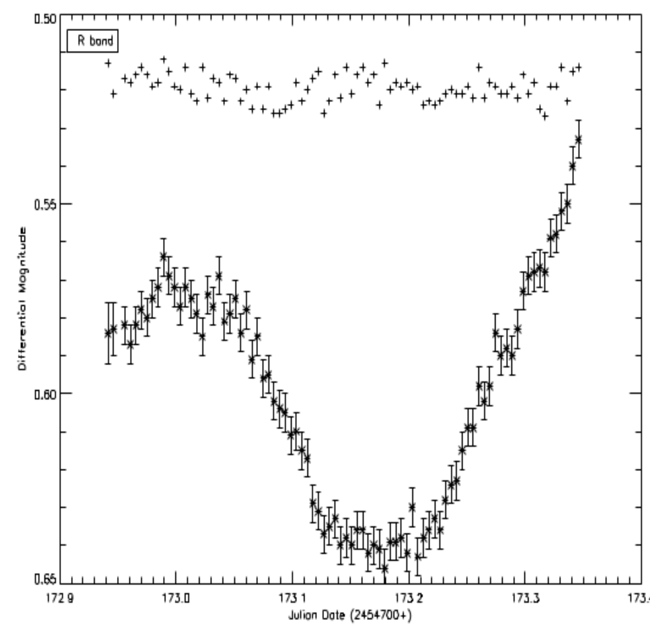

5-day multi-frequency photo-polarimetric WEBT campaign on blazar S5 0716+714

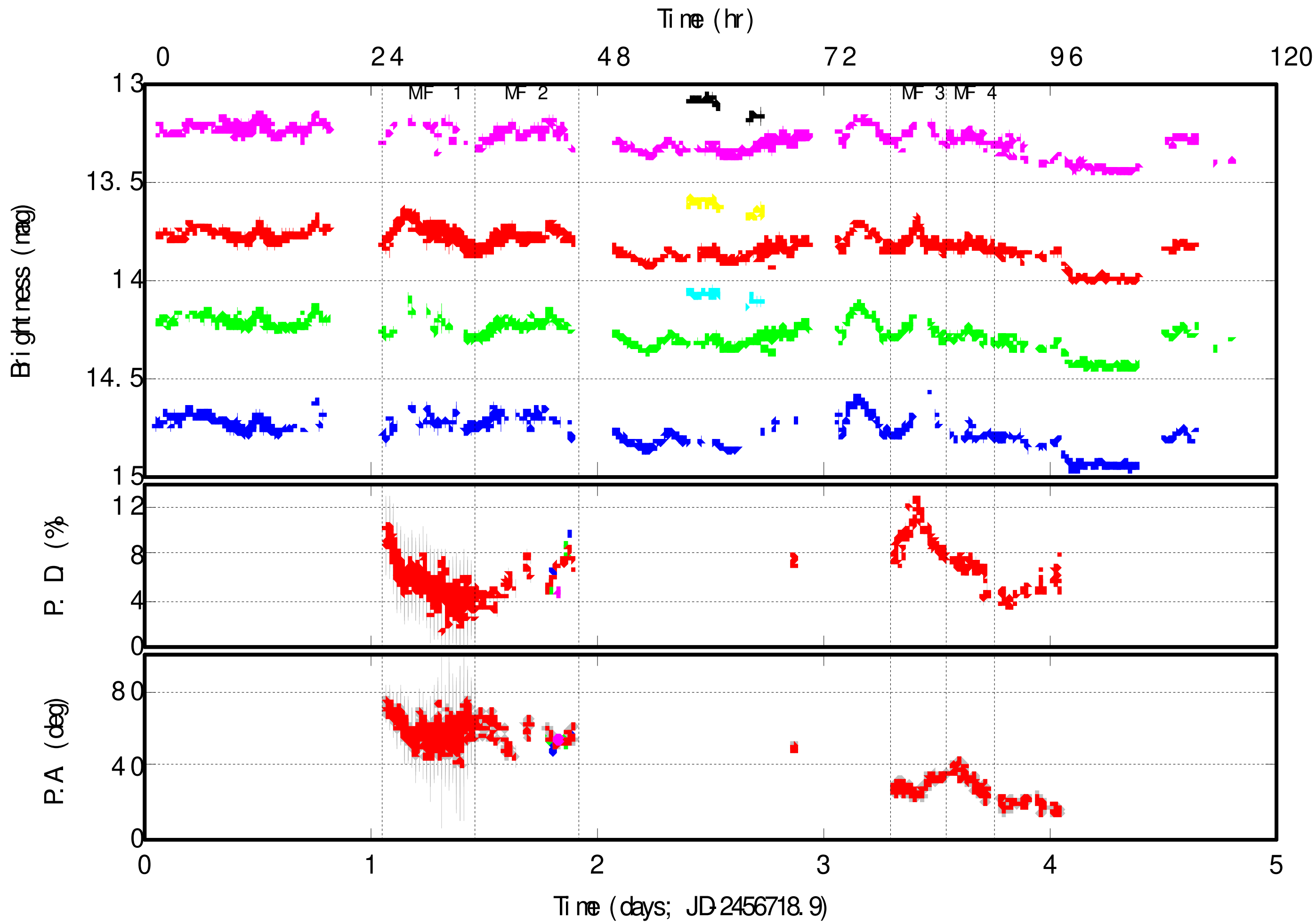

Bhatta et al. 2016 ApJ

Photometric Observations – BVRI bands

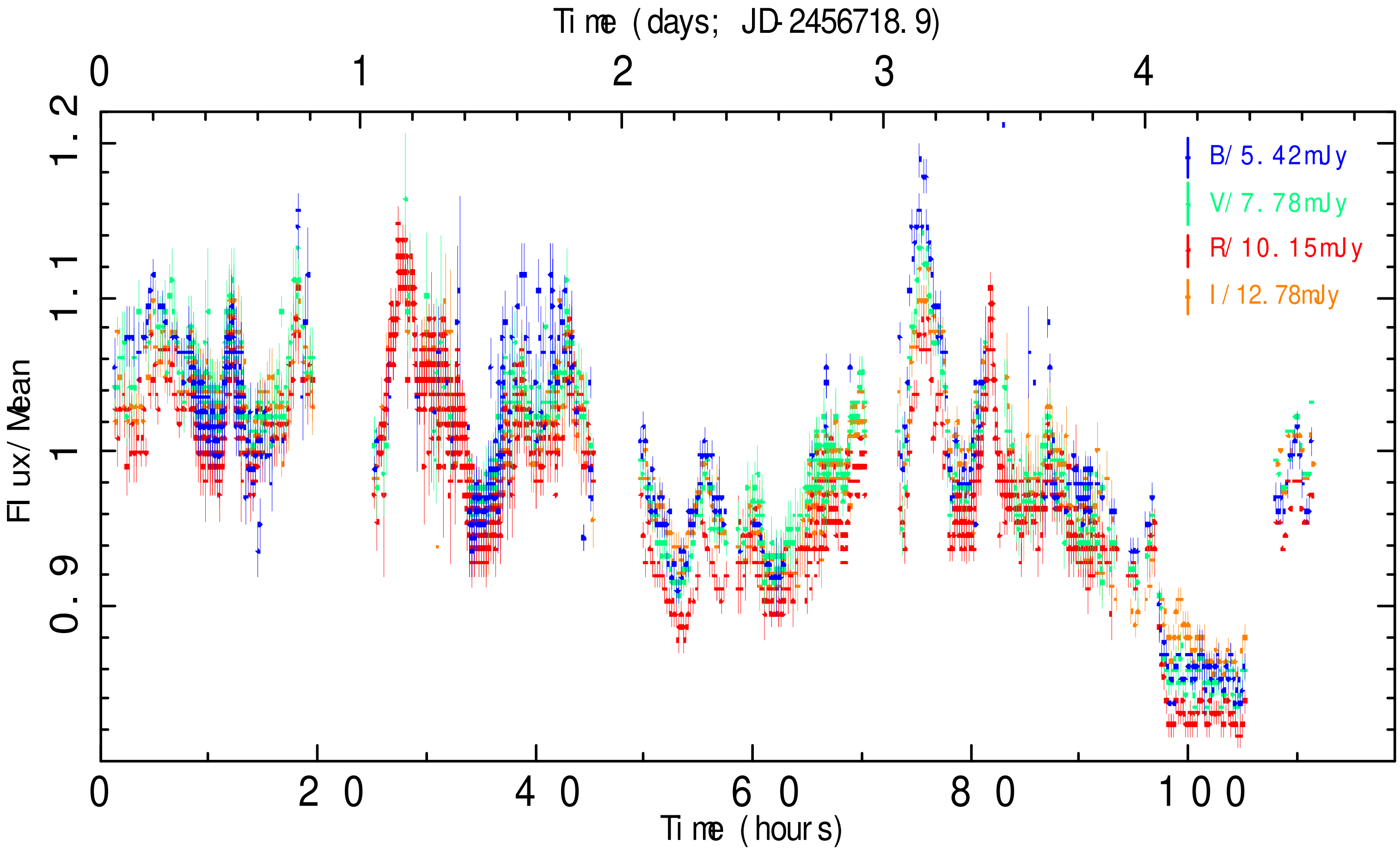

Periodicity search and red-noise PSD

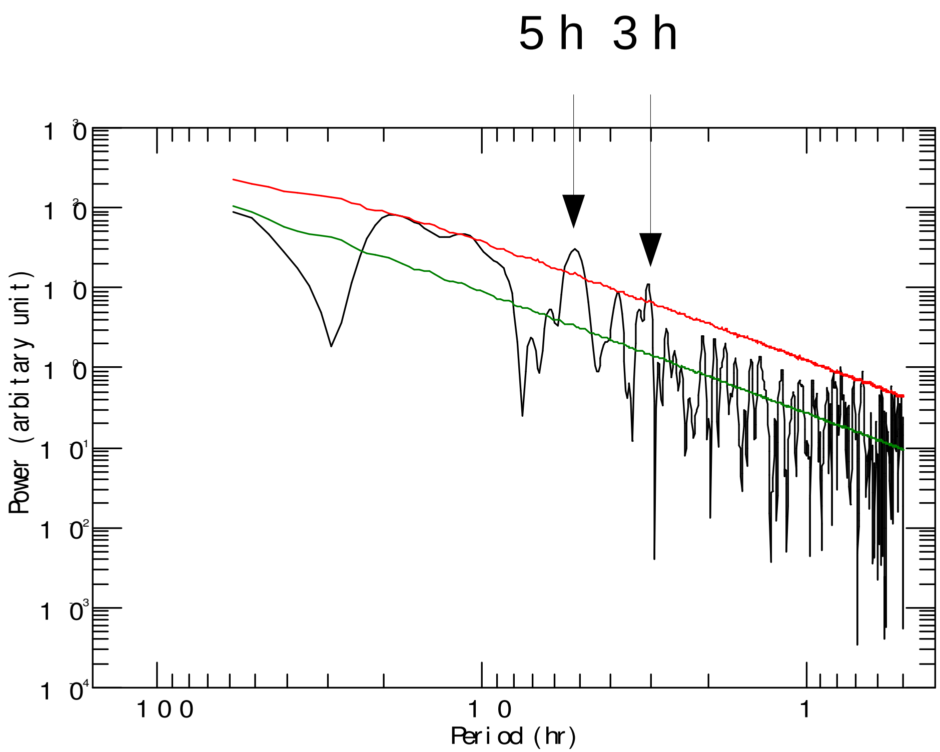

Lomb-Scargle periodogram (black), mean simulate periodogram (green) and 99% confidence contour from the simulations (red)

Hints for the presence of quasi- periodic oscillations at timescales of 3 h and 5 h were seen.

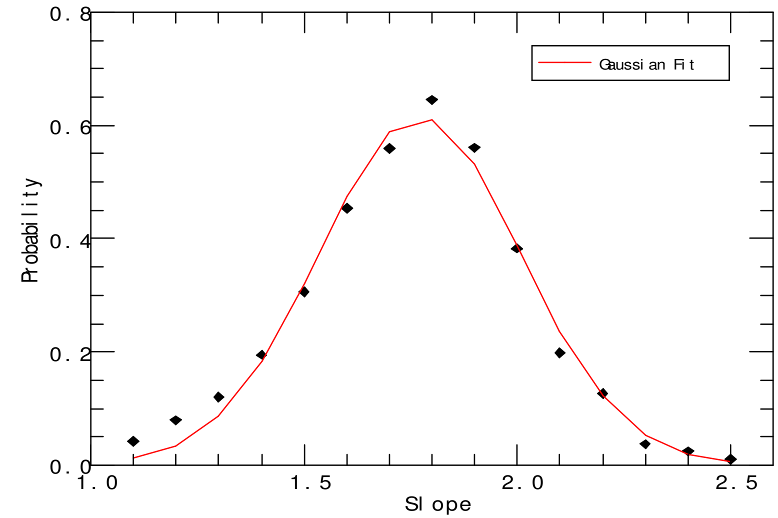

Probability that the power-law slope is acceptable

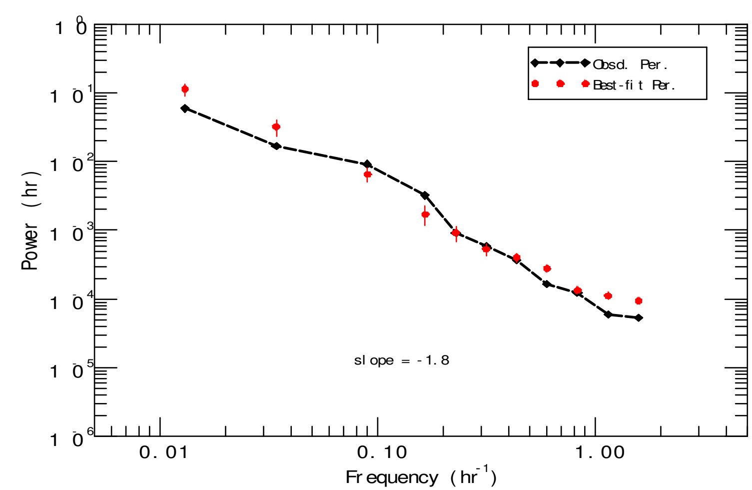

Binned PSD and the best-fit model

The Plateau - Jet Activity Choked ?

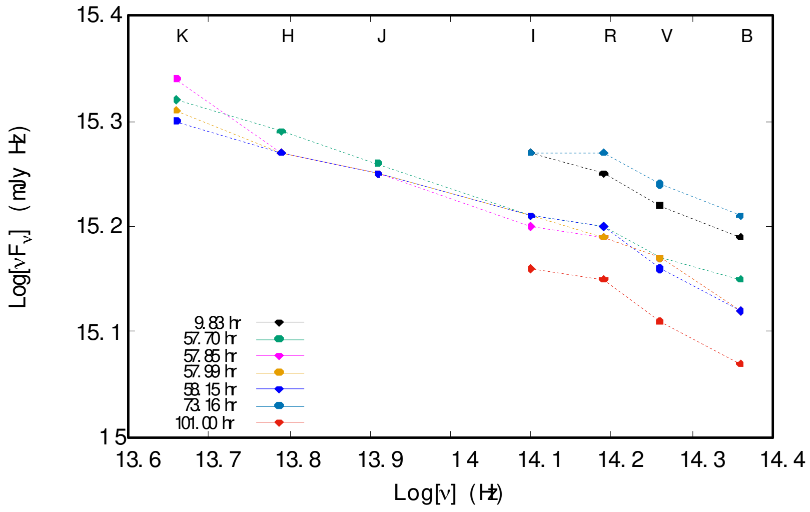

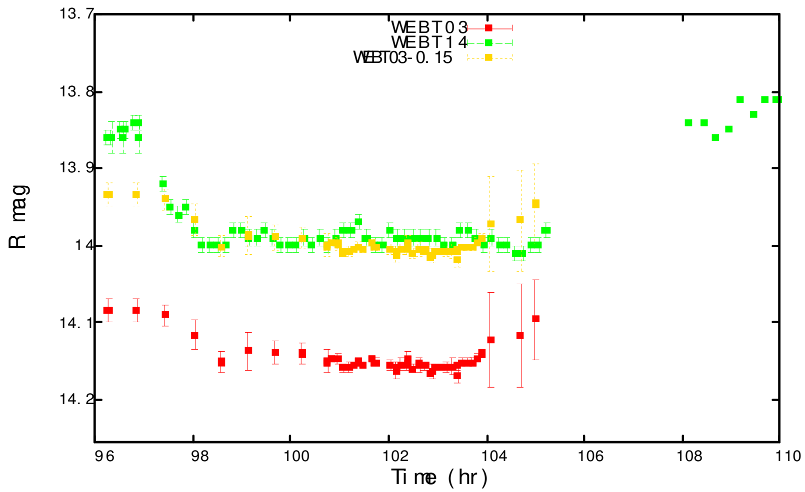

The optical spectra during the campaign.

Keplerian Period around the ISCO

$$\tau_K = \tau_g \left(\frac{r_{isco}}{r_g}\right)^{3/2} \simeq 500 \left(\frac{\mathcal{M}}{10^8 M_\odot}\right) \left(\frac{r_{isco}}{r_g}\right)^{3/2} \text{ s}$$

$$\tau_g = r_g/c = G\mathcal{M}/c^3$$

This could be result of temporarily suppressed flow at the jet base !!

$\mathcal{M} \simeq 3 \times 10^8 M_\odot$ assuming very low spin values ($r_{isco} \simeq 6\, r_g$)

Color (B-I) Variability

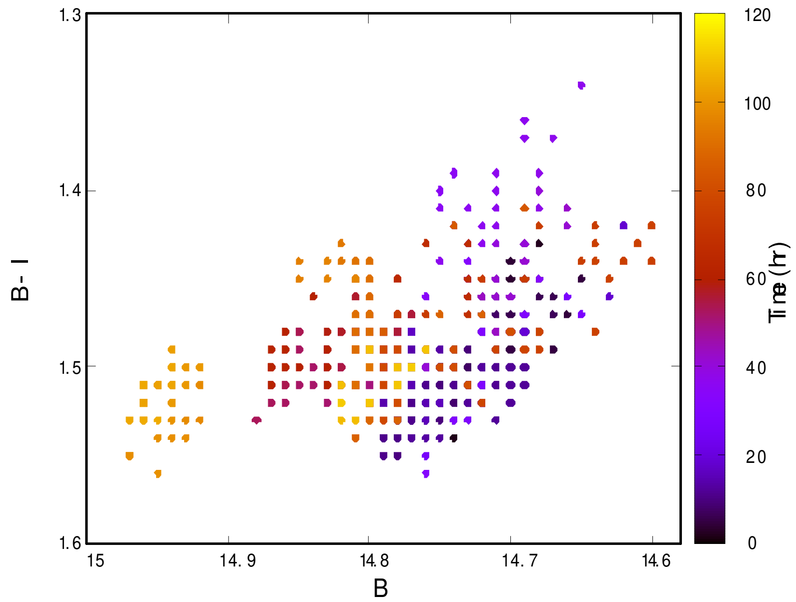

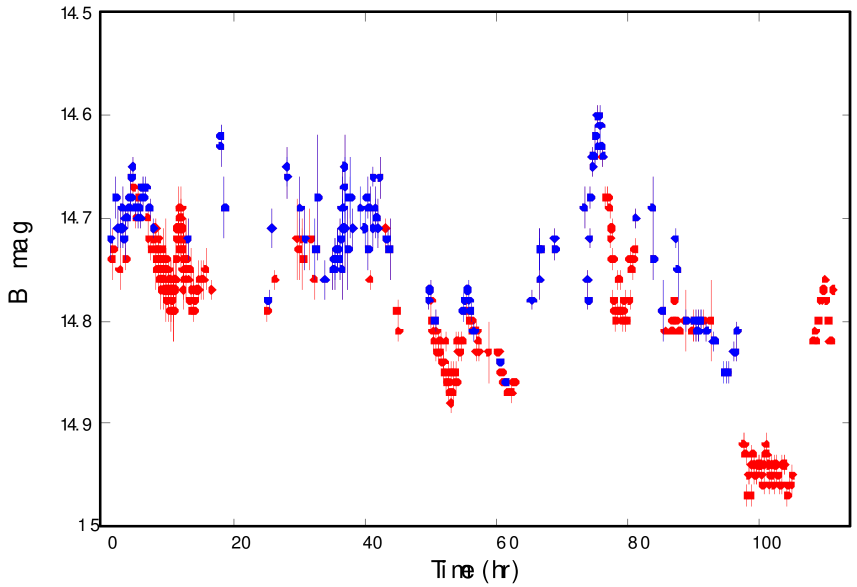

Bluer-when-brighter" trend was observed in the color-magnitude diagram

the B-band light curve color coded with high (blue) and low (red) color value.

B- and I-band Cross-Correlation

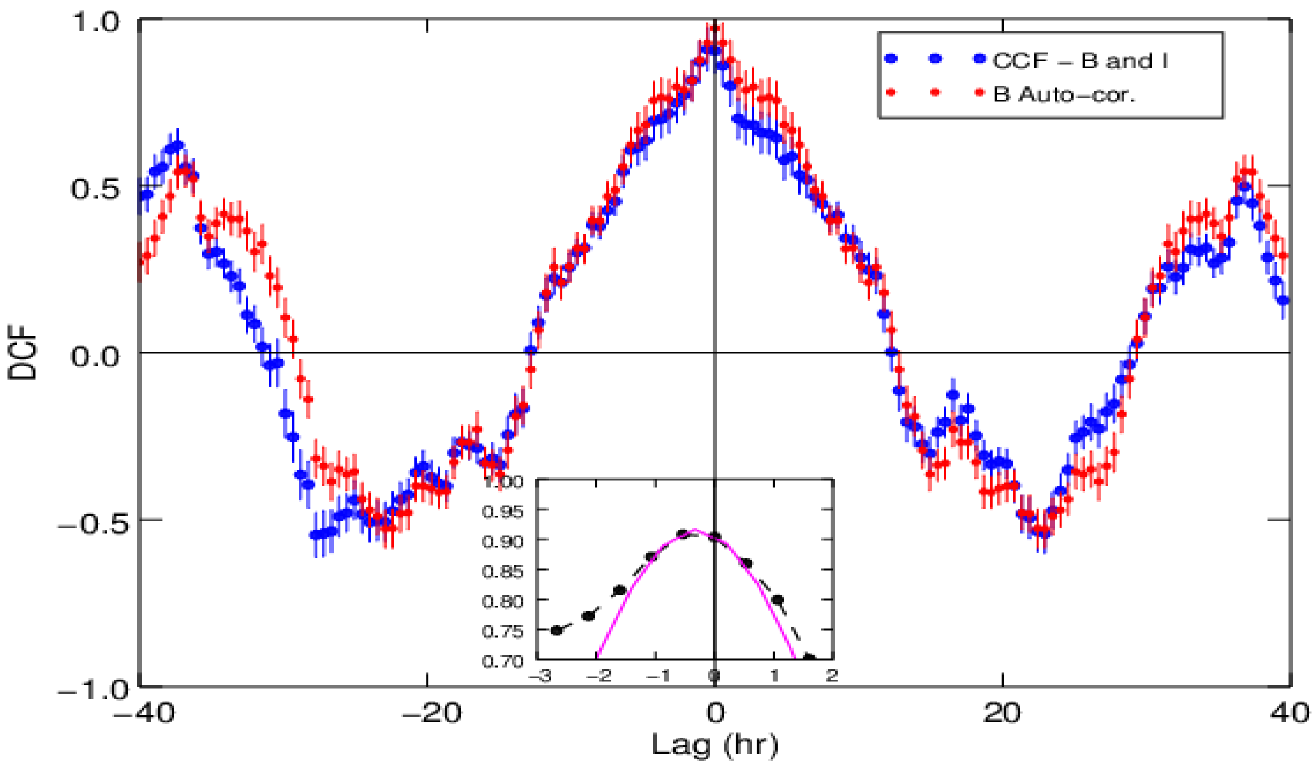

B- and I-band emission are highly correlated at large with a small possible lead of HE emission over LE emission

Epoch I:Flux-PD-PA Correlation

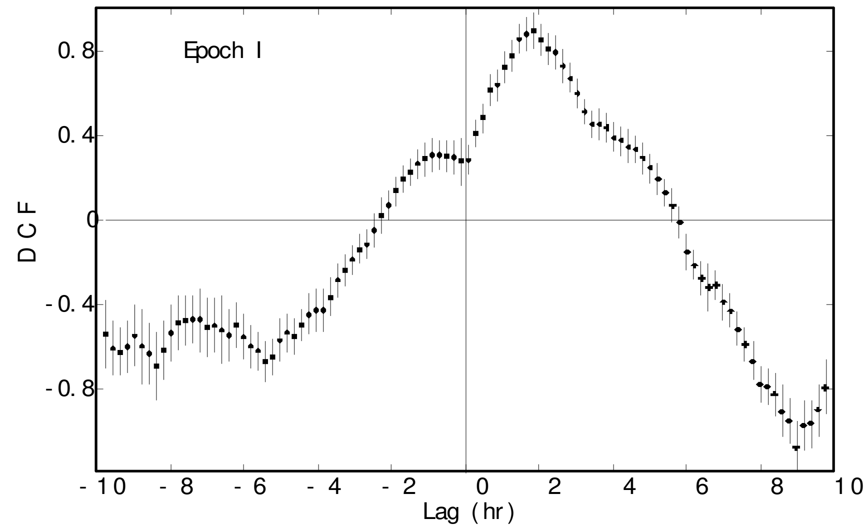

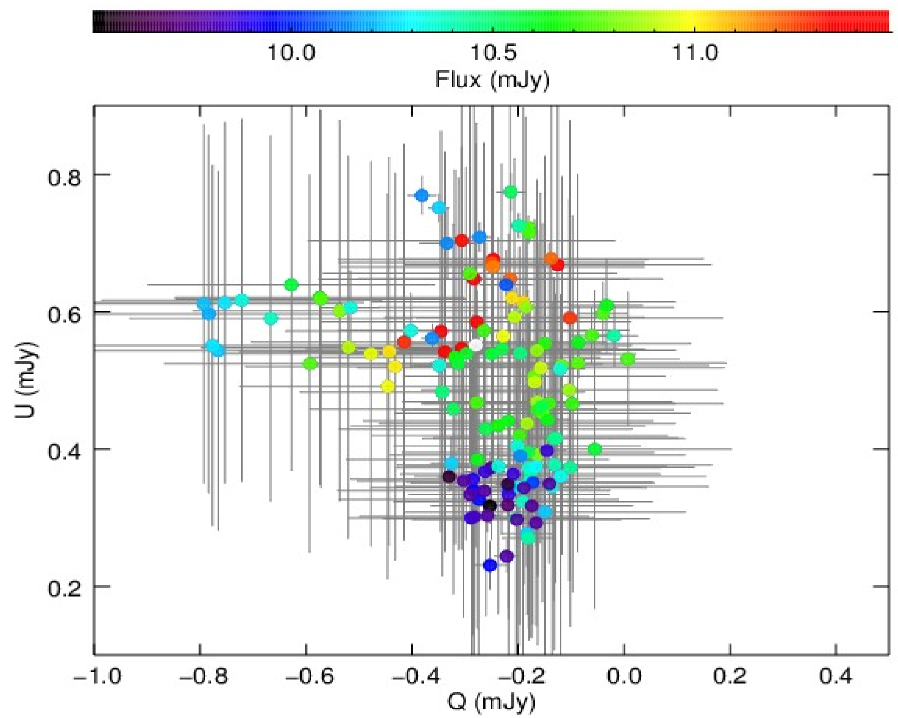

The evolution of Stokes parameters Q and U during Epoch I

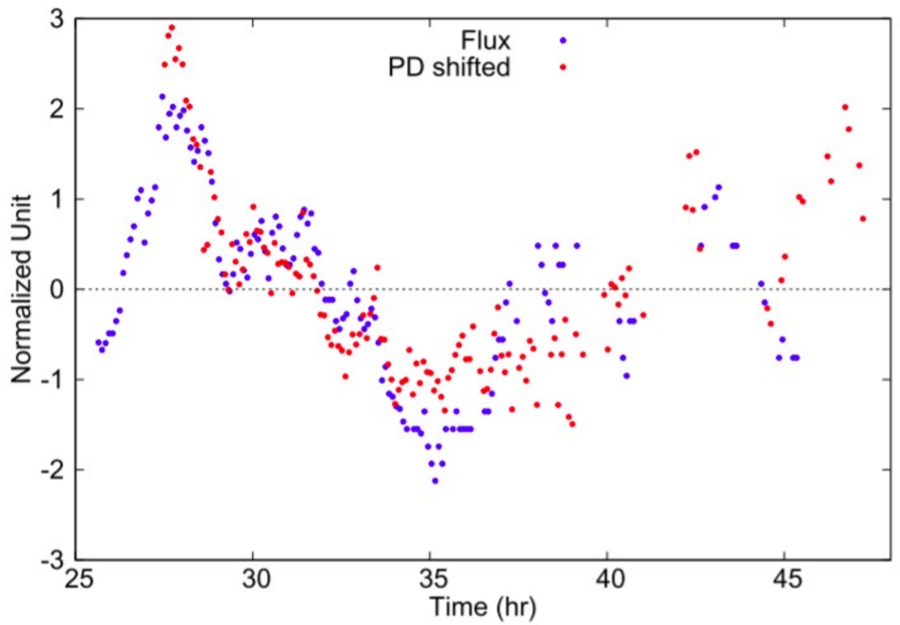

The discrete correlation function between flux and PD shows flux lagging behind PD by 2 hrs (above). It can be also be seen in normalized flux and PD shifted by 2 hrs (below)

Epoch II: Flux-PD-PA Correlation

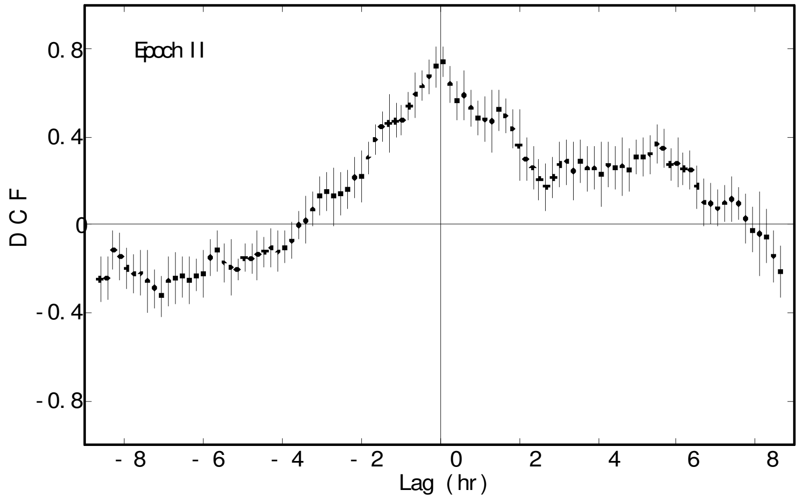

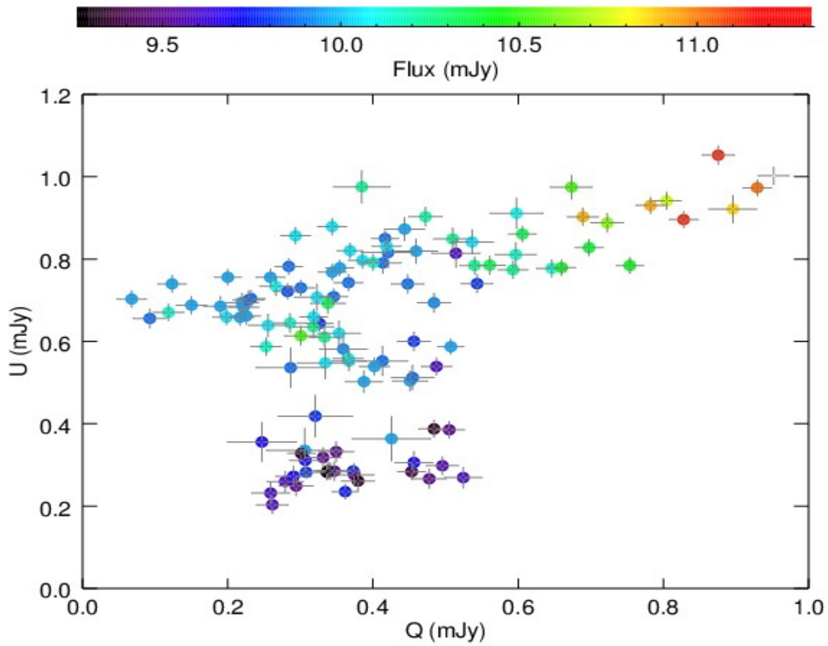

The evolution of Stokes parameters Q and U during Epoch II

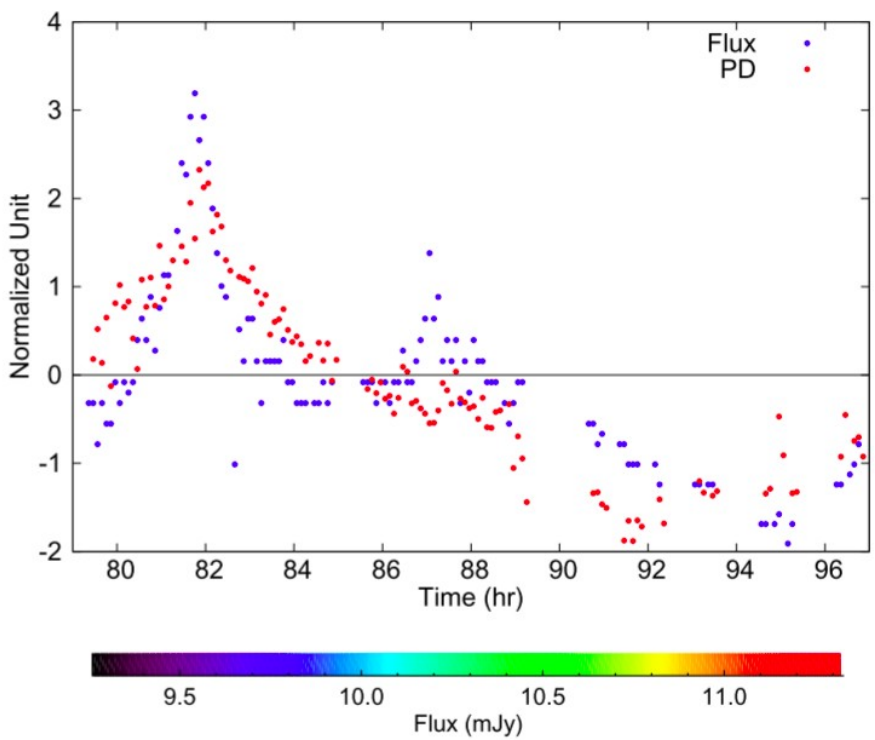

The discrete correlation function between flux and PD showing high correlation (above). It can be also be seen in normalized flux and PD (below).

Modeling of Individual Microflares

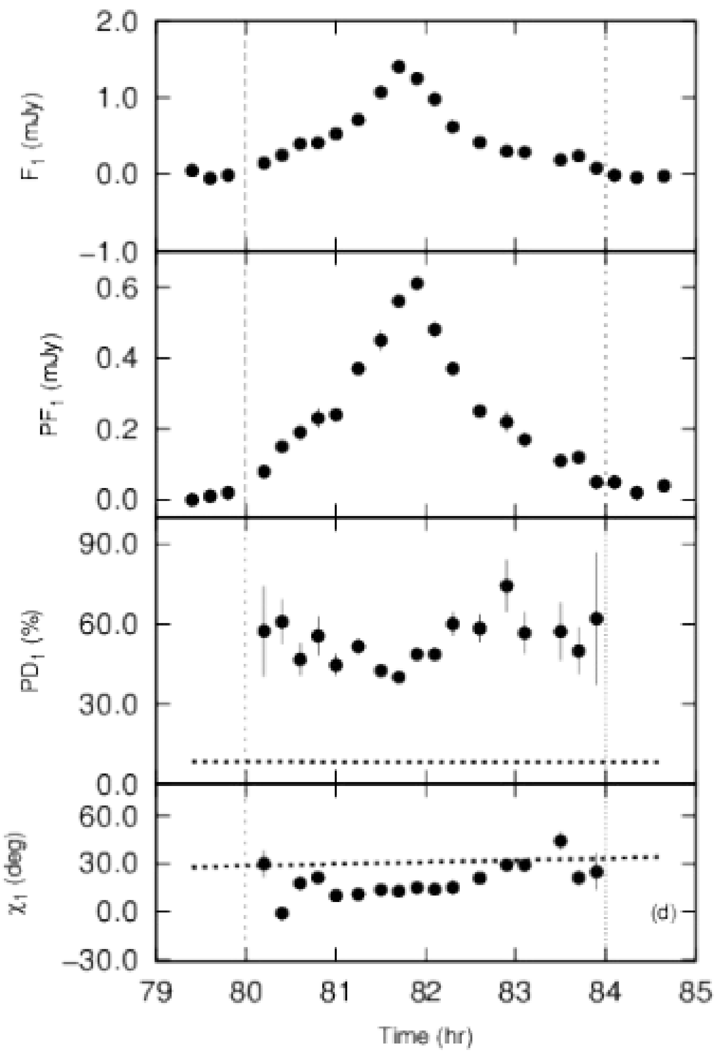

The modeling shows presence of highly polarized microflares during the campaign

Bhatta et al. 2015, ApJL, 09, L27

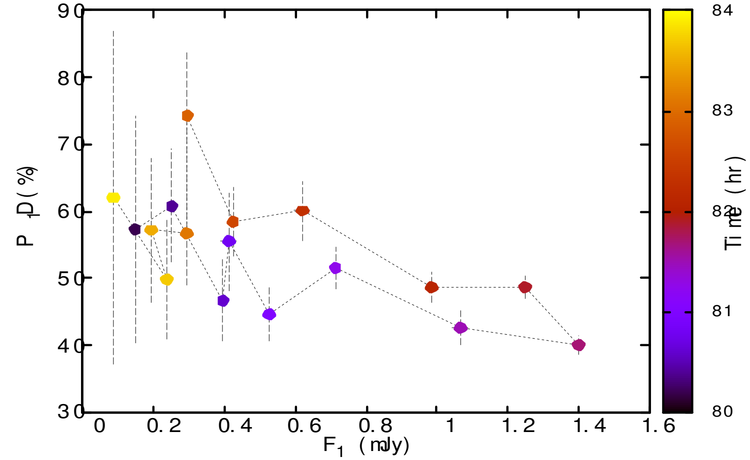

The modeled flux and PD for the flaring component appear in anti-correlation

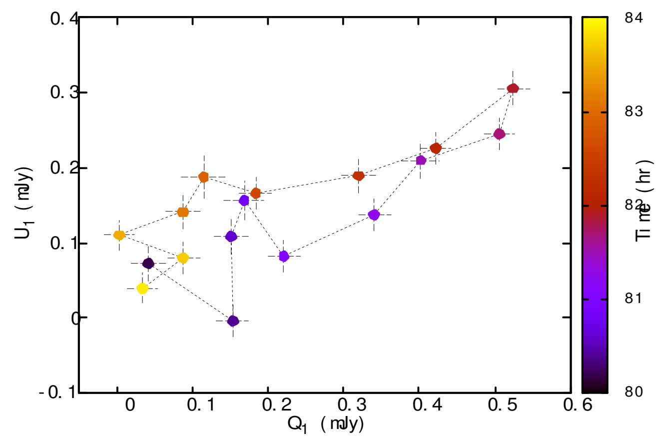

The flaring component exhibits loop-like behavior in the Q-U plane

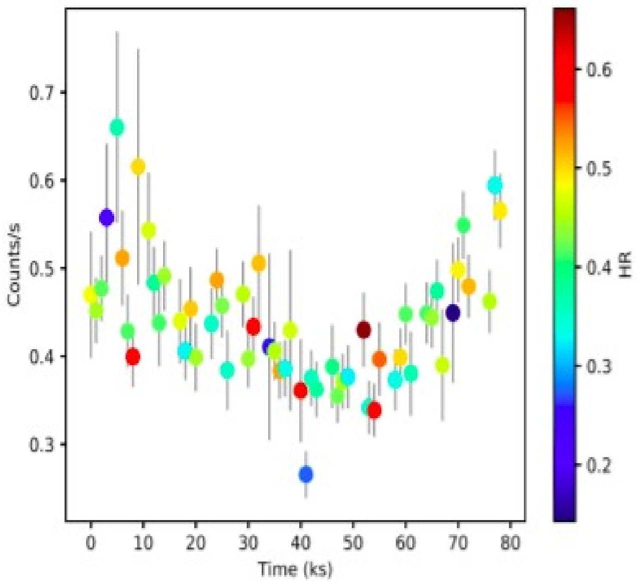

3C 279, 60002020002

NuSTAR telesope: timing and spectral analysis of blazars in the hard X-ray band

Bhatta, et al. 2018, A&A, 619, A93

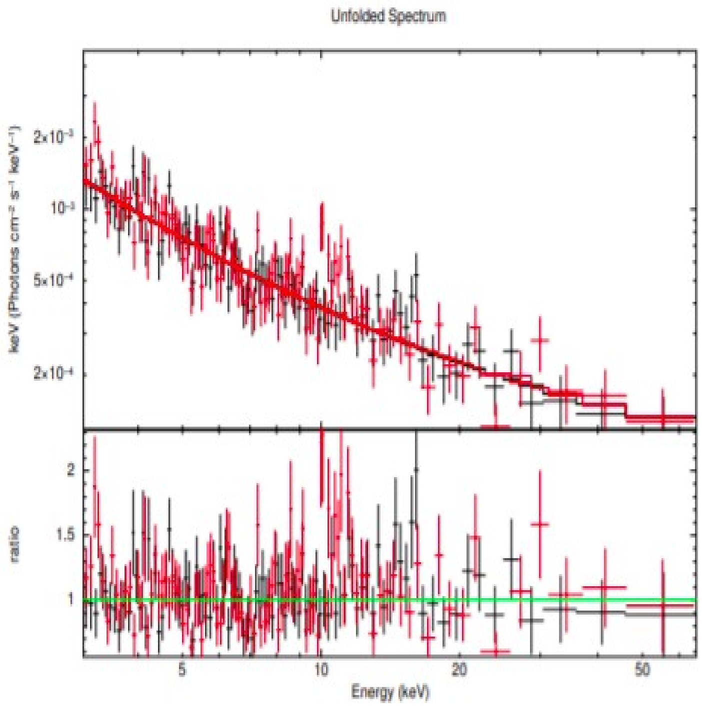

S5 0716+714, 90002003002

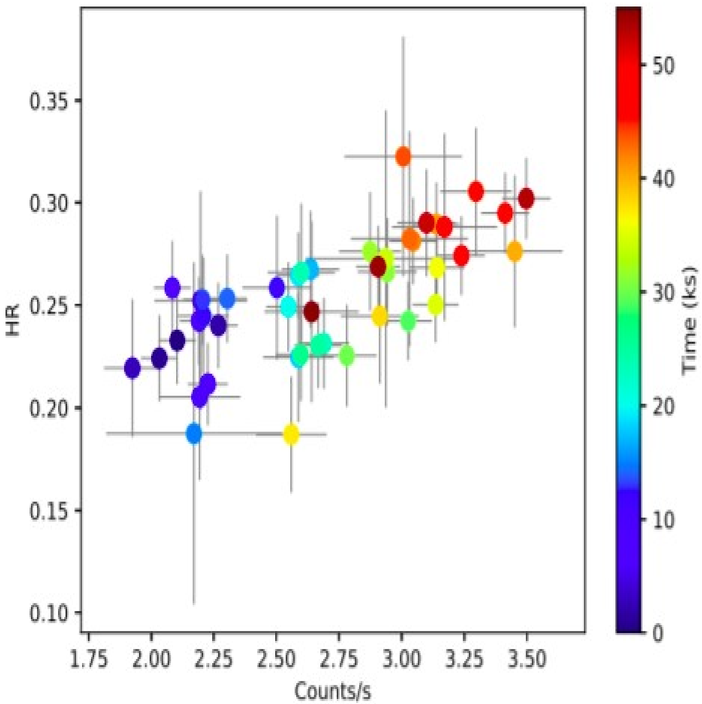

Mrk 501, 60002024004

Hard X-ray properties of blazars

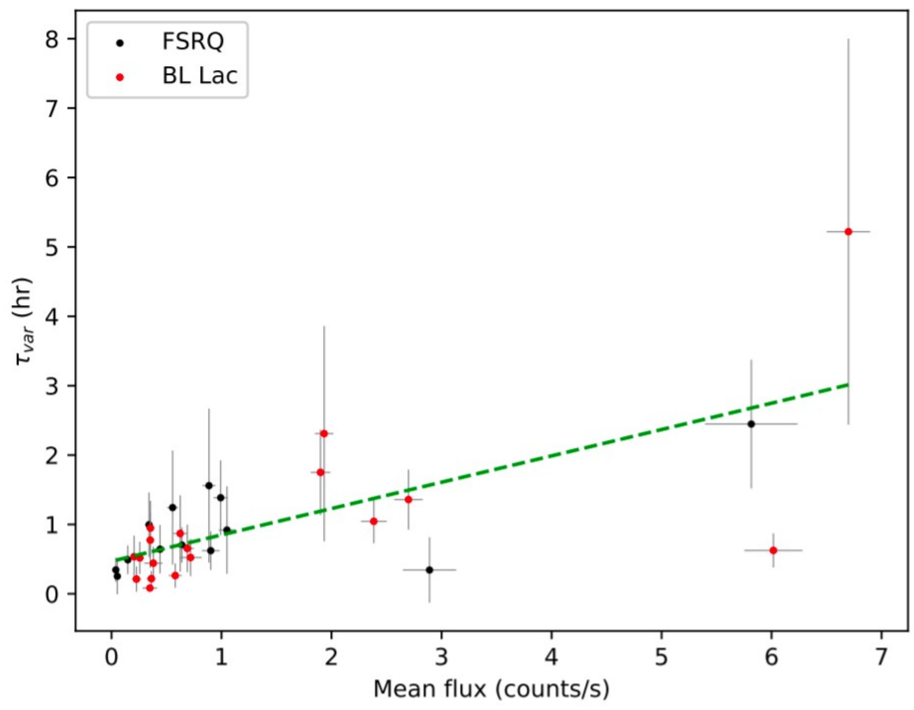

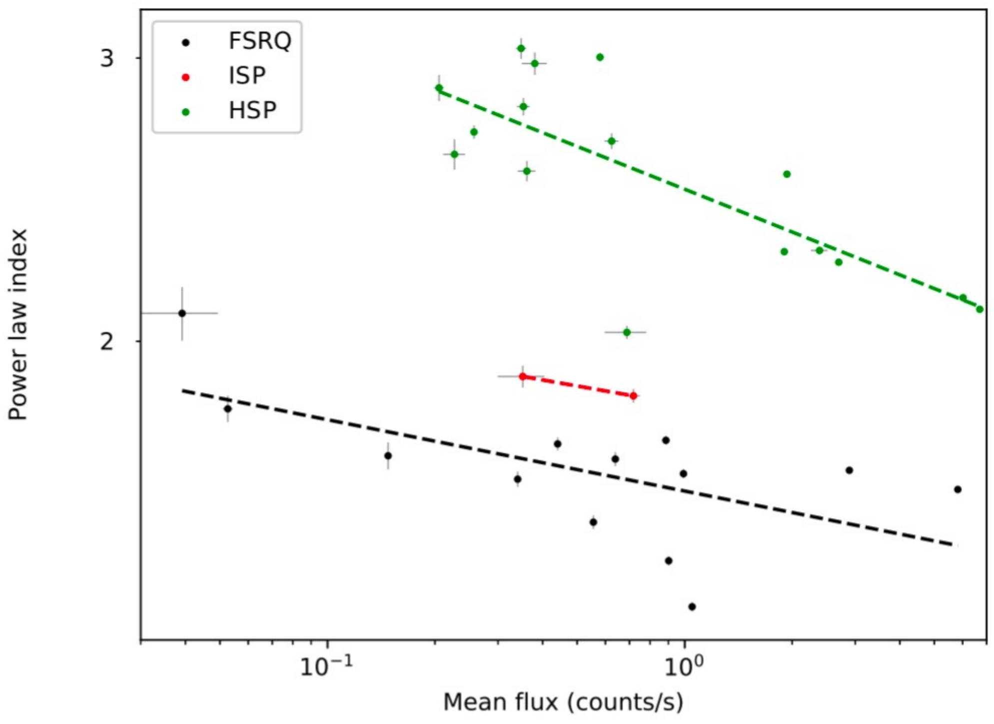

Bhatta, et al. 2018, A&A, 619, A93

The nature of gamma-ray variability in blazar

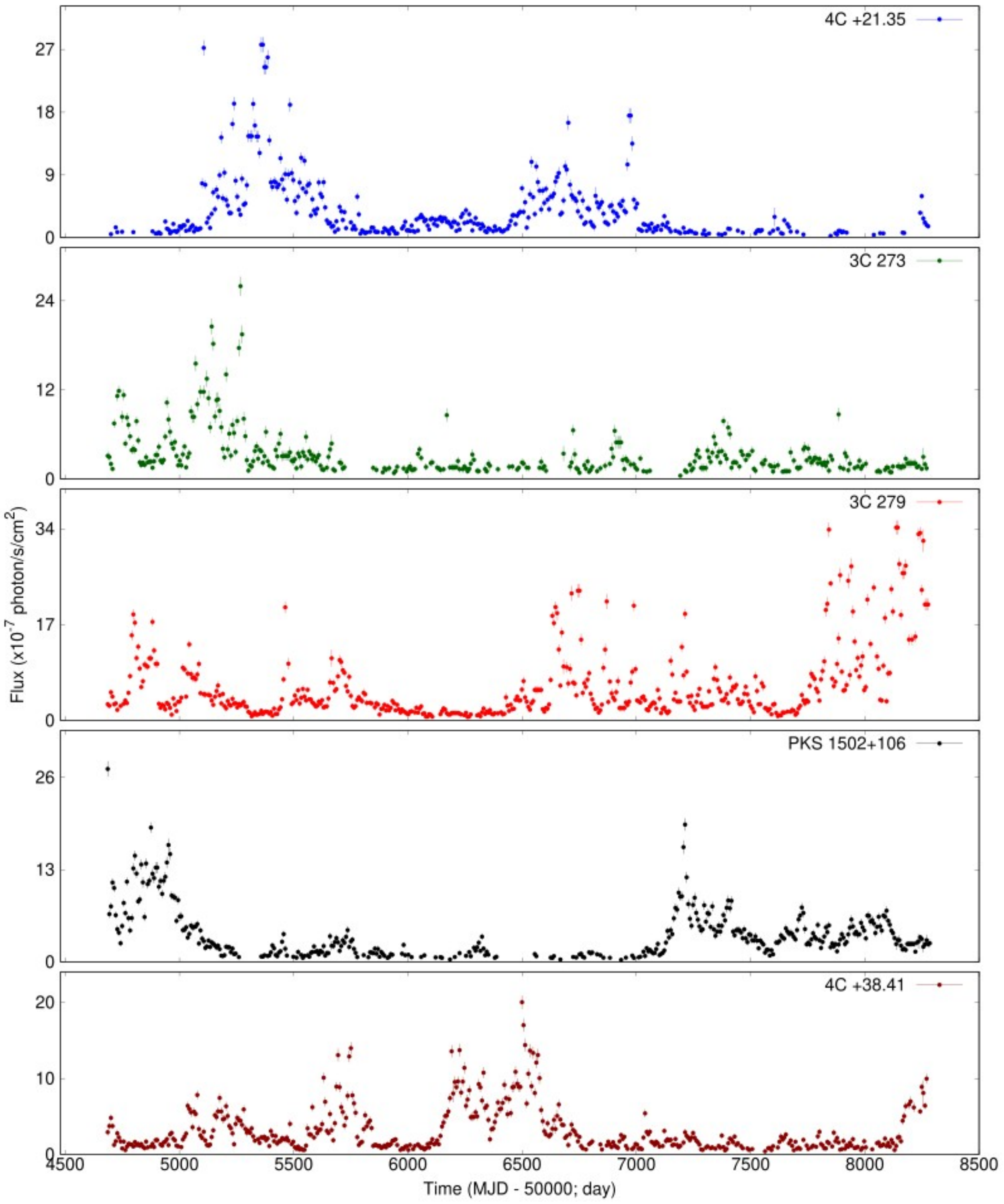

Flux distribution: probability distribution function

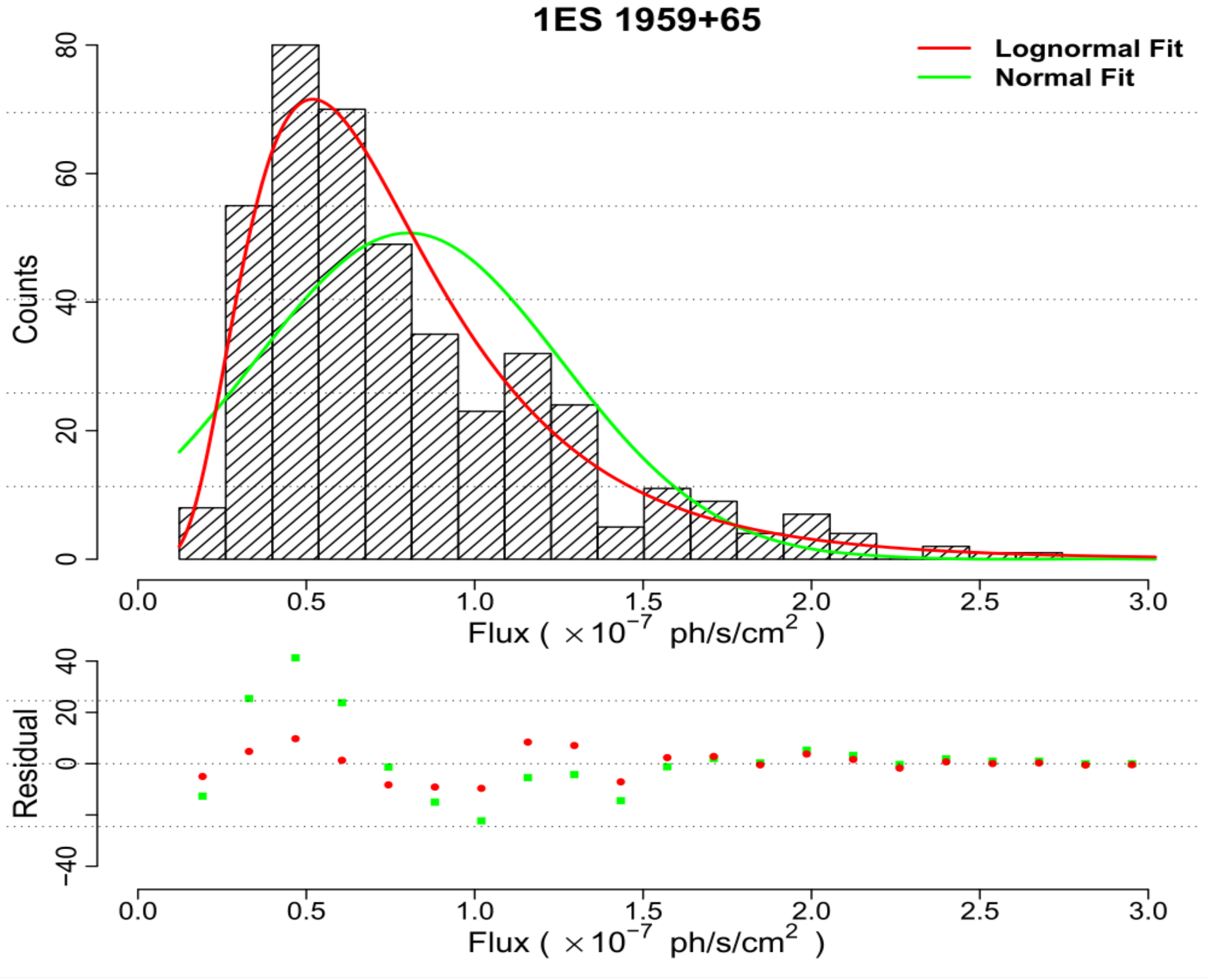

Power spectral density: flicker noise, long memory processes

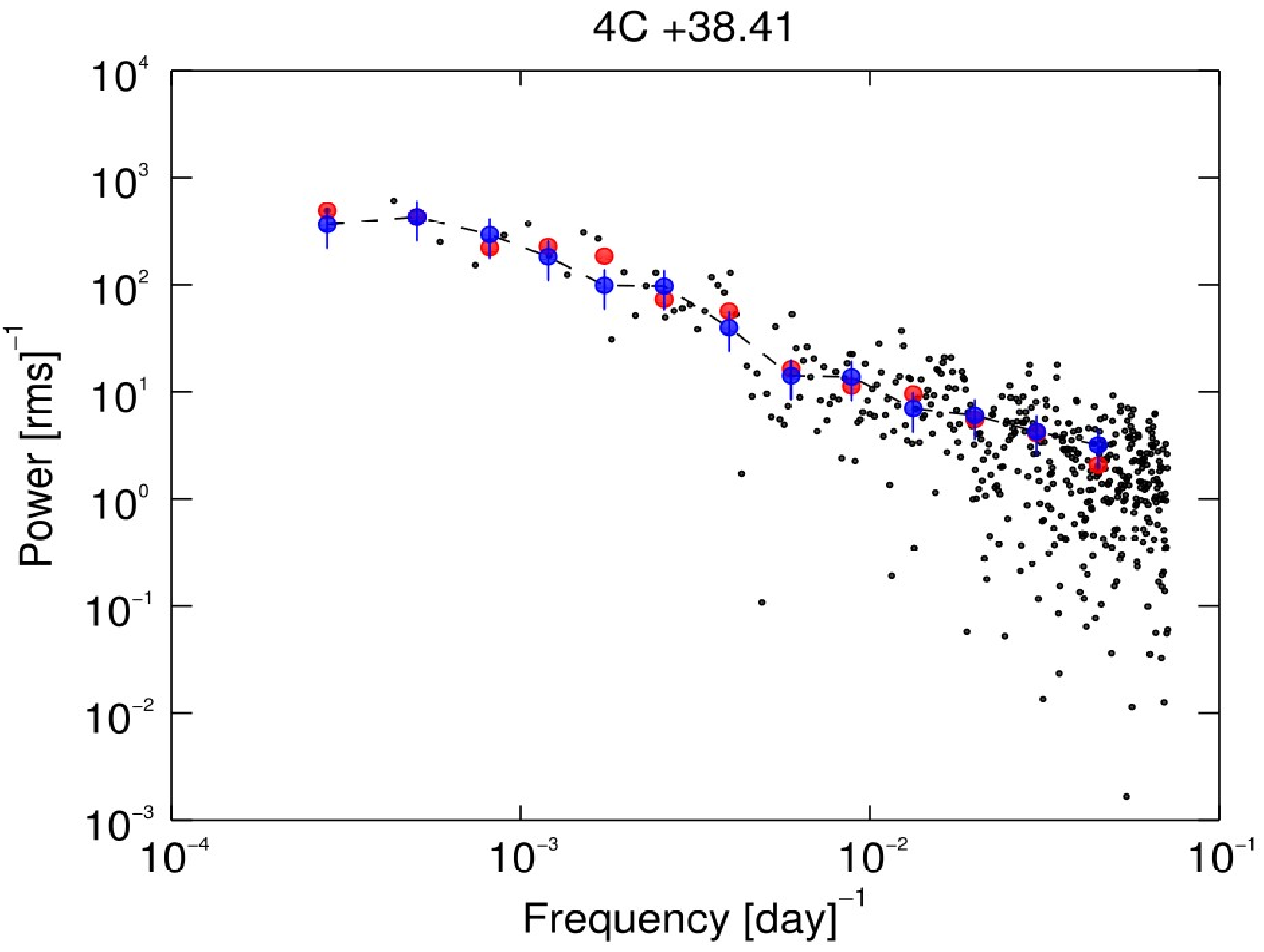

Linear RMS-Flux relation

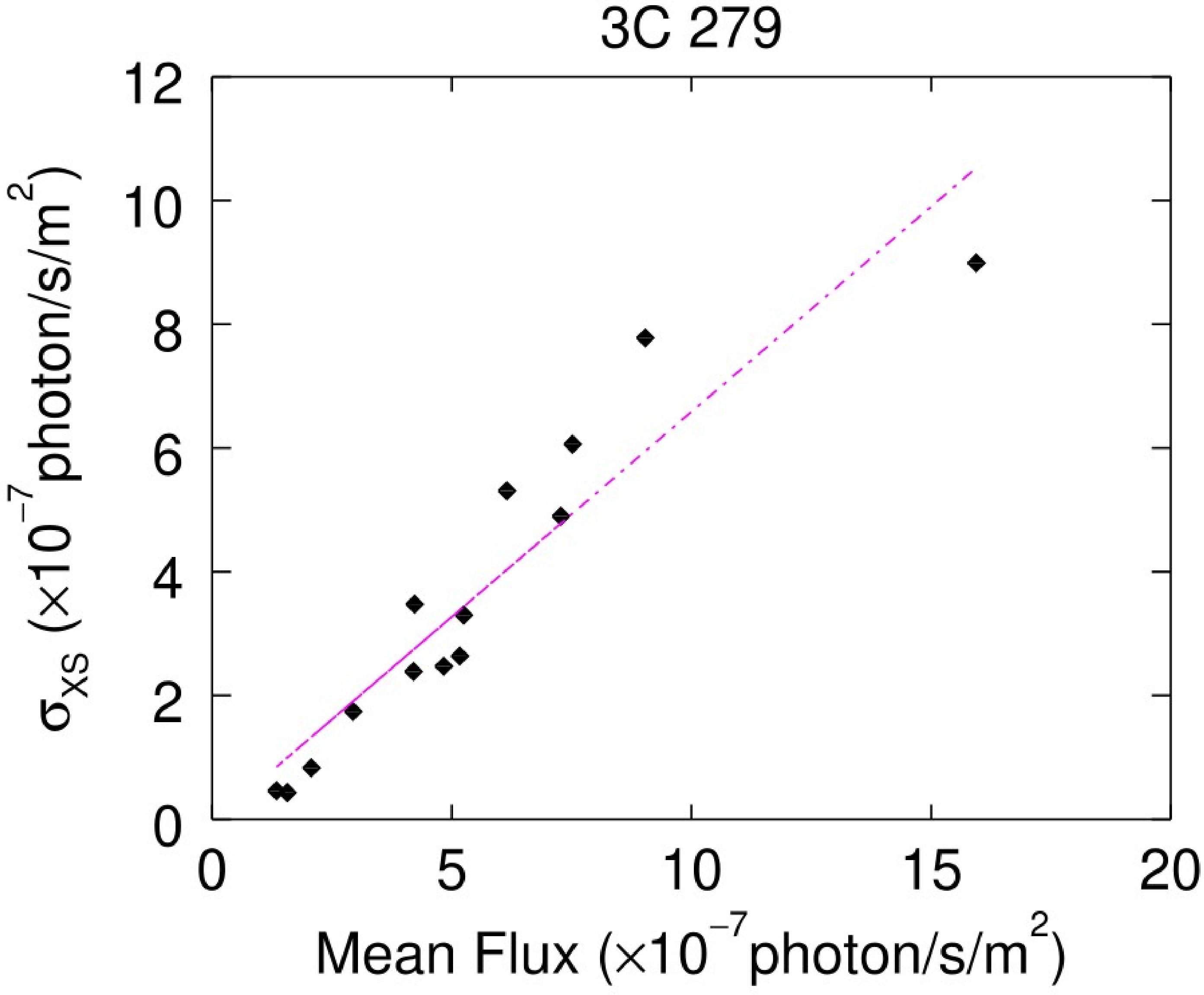

Summary

I. the overall variability of the source is of the red noise type, flicker noise (consistent with a random-walk long-memory process).

II. Hints for quasi-periodic oscillations at timescales of ∼3h and ∼5h were found as well, though there are indications that they do not represent highly significant departures from a pure red-noise power spectrum.

III. The observed optical flux is produced in compact emission sites within the outflow, with range of sizes and range of distances from the core;
 - only sometimes polarization properties reveal any coherence in the magnetic field evolution (e.g. PD leading the total flux changes, hysteresis in the PD-F plane, large PA swings, etc.).

IV. Compact emission sites may be identified with either turbulent cells, merging magnetic island related to magnetic reconnection, or small-scale internal shocks.

V. In hard X-ray regime, the spectra can be well represented by log-parabola model; minimum variability timescale correlation with flux states, and “harder-when-bright” trend is observed’

VI. In the gamma-ray band, remarkable variability, lognormal processes, PSD reveals the signs of long memory process, linear RMS-Flux is observed.

Quasi-periodic oscillations in blazars

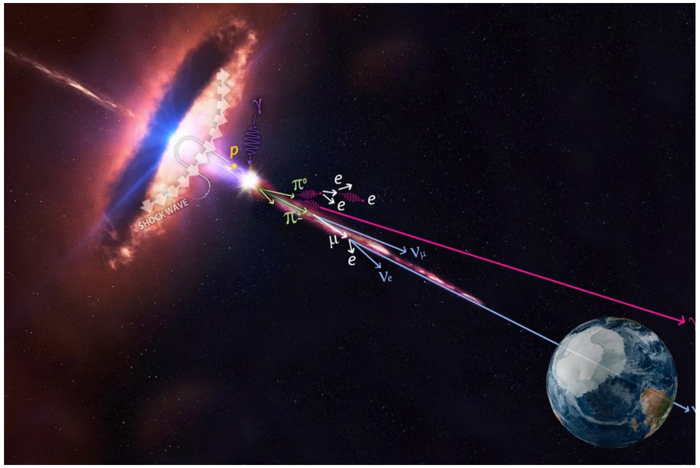

- (Quasi) Periodic signal from X-ray binary

  are well established.

  However, QPOs in blazar or in general AGN are subjects of Intense debate.

- The year-scale QPOs are reported in many works are of the marginal significance

- Gaps in the temporally limited astronomical observations

- The QPOs often last on a few cycles before they fade away

- The low frequency QPOs are hard to distinguish from the red-noise which is dominant in the blazar light curve

Best examples of periodic oscillations blazar

~12 year optical QPO in the historical (from year 1980 to 2005) light curve of the blazar **OJ 287**

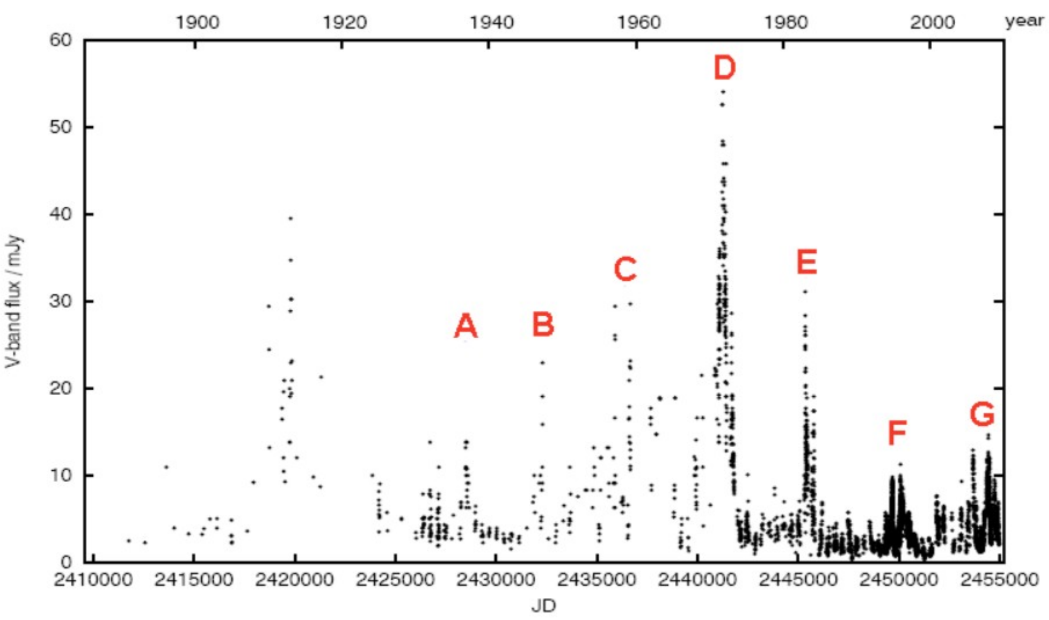

Sillanpää et al. 1988

2 year gamma-ray QPO in the blazar **PG 1553+113** observed in the ~7 years Fermi/LAT observations

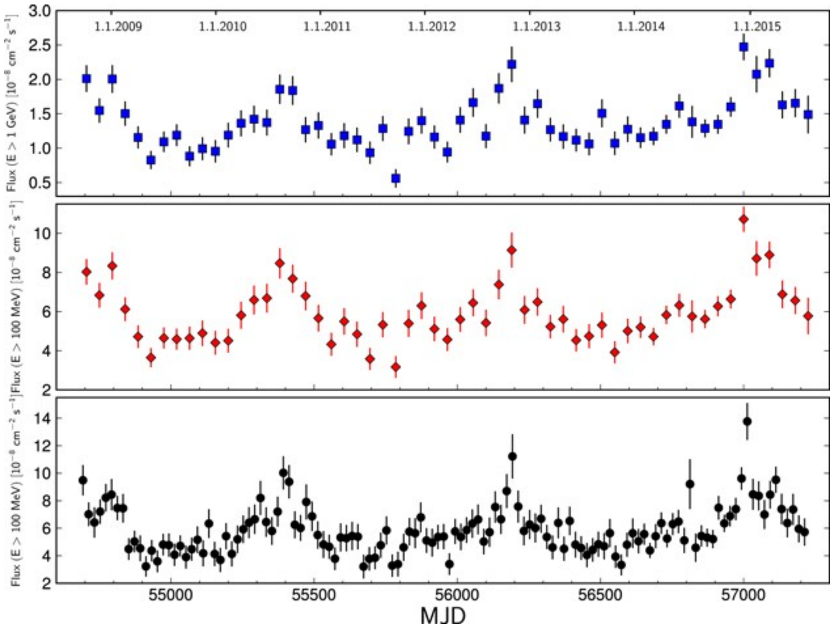

Ackermann, 2015ApJ, 813L, 41A

Motivation

- Search for binary supermassive black holes in AGN and thereby possible sources of low-frequency gravitational waves.
- Study disk-jet connection in blazars
- Understating of the physical processes at the innermost regions of radio-loud galaxies including ejection of relativistic jets and accretion around super massive black hole
- Investigate the nature of space-time under extreme gravity conditions such as around fast rotating supermassive black holes.

Methods of time series analyses

- Frequency domain based analyses:
  - Discrete Fourier periodogram $$P(\nu) = \frac{2\,T}{(N\bar{f}\,)^2} \left| \sum_{j=1}^{N} f(t_i)\, e^{-i2\pi\nu t_j} \right|^2$$
  - Lomb-Scargle periodogram $$P = \frac{1}{2}\left\{ \frac{\left[\sum_i x_i \cos\omega\,(t_i - \tau)\right]^2}{\sum_i \cos^2\omega\,(t_i - \tau)} + \frac{\left[\sum_i x_i \sin\omega\,(t_i - \tau)\right]^2}{\sum_i \sin^2\omega\,(t_i - \tau)} \right\} \quad \tan(2\omega\tau) = \frac{\sum_i \sin\omega t_i}{\sum_i \cos\omega t_i}$$
  - Weighted wavelet z-transform $$\phi_2 = \cos\left[\omega\,(t - \tau)\right] \quad \phi_2 = \sin\left[\omega\,(t - \tau)\right] \quad \phi_1(t) = 1(t)$$
- Time Domain based analyses:
  - Auto-correlation function $$UDCF_{ij} = \frac{(x_i - \bar{x})\,(y_j - \bar{y})}{\sqrt{(\sigma_x^2 - e_x^2)\,(\sigma_y^2 - e_y^2)}} \qquad DCF(\tau) = \frac{1}{M} UDCF_{ij}$$
  - Epoch folding $$\chi^2 = \sum_{i=1}^{M} \frac{(x_i - \bar{x})^2}{\sigma_i^2}$$

Significance estimation: PSRESP

Challenges of astronomical time series analyses

- Red noise
- Uneven sampling Gaps in the observations
- Finite duration observation
- Aliasing

Power Spectrum Response (PSRESP) method takes account of most of the above problems.

- Find the model PSD to fit the observed periodogram
- Using this model simulate a large number of light curves with the same sampling of the observations.
- Estimate the significance of the observed QPO against spurious detection

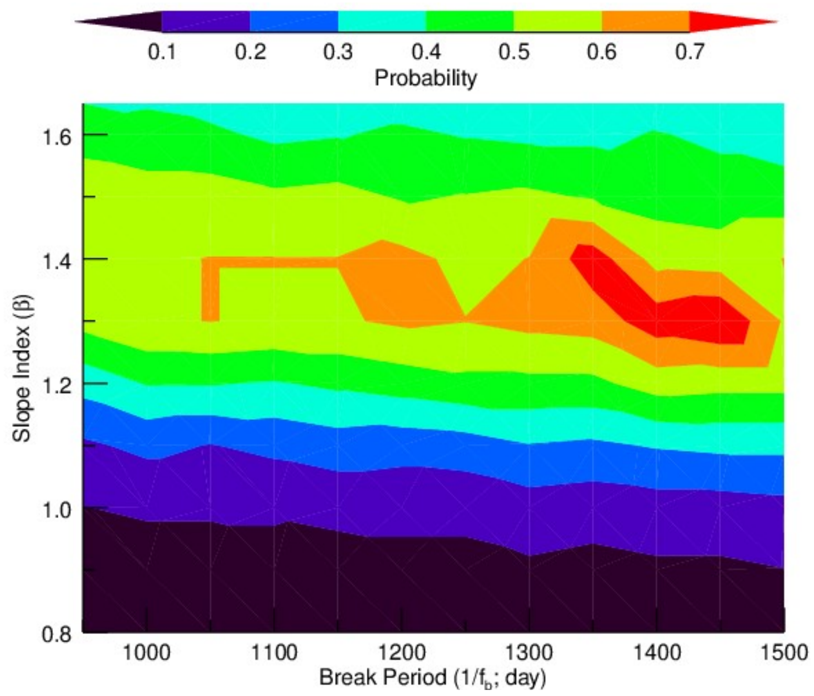

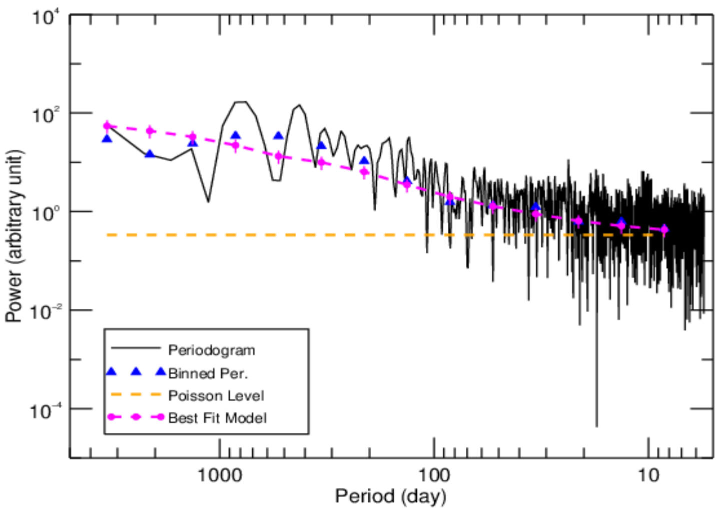

Bhatta, G. 2016, ApJ, 832, 47B

400-day Optical QPO in blazar OJ 287

Bhatta, G. 2016, ApJ, 832, 47B

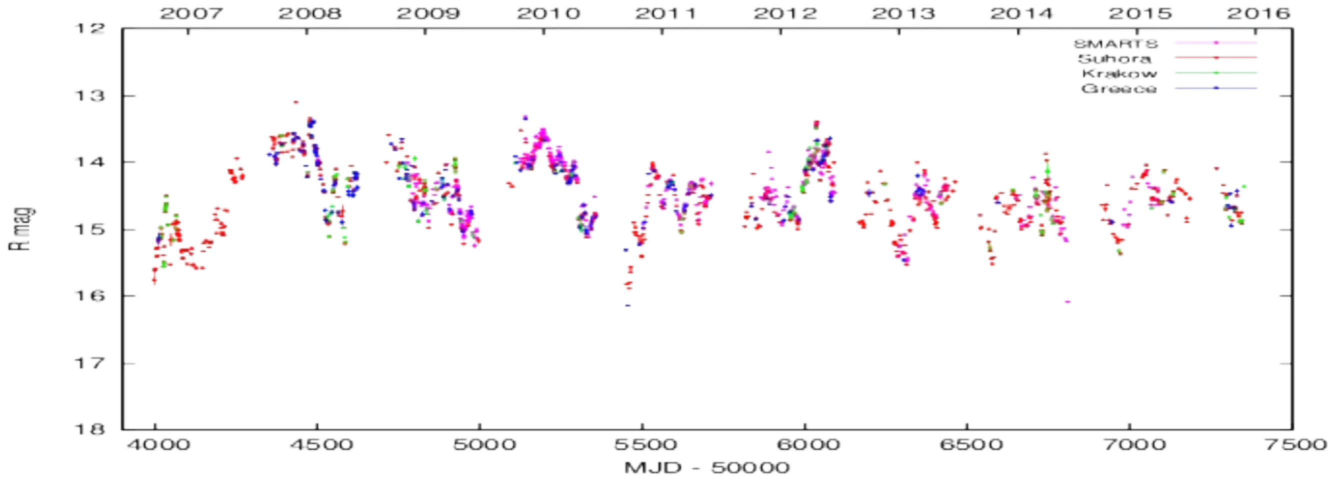

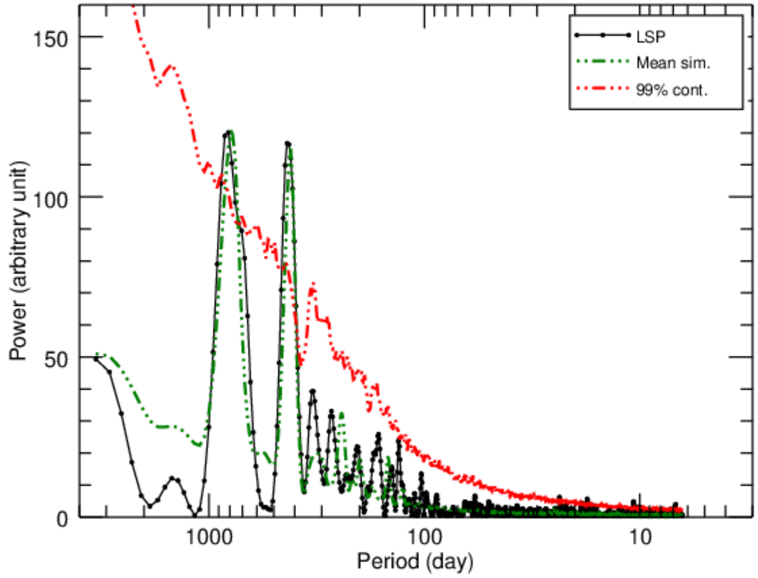

Lomb-Scargle periodogram

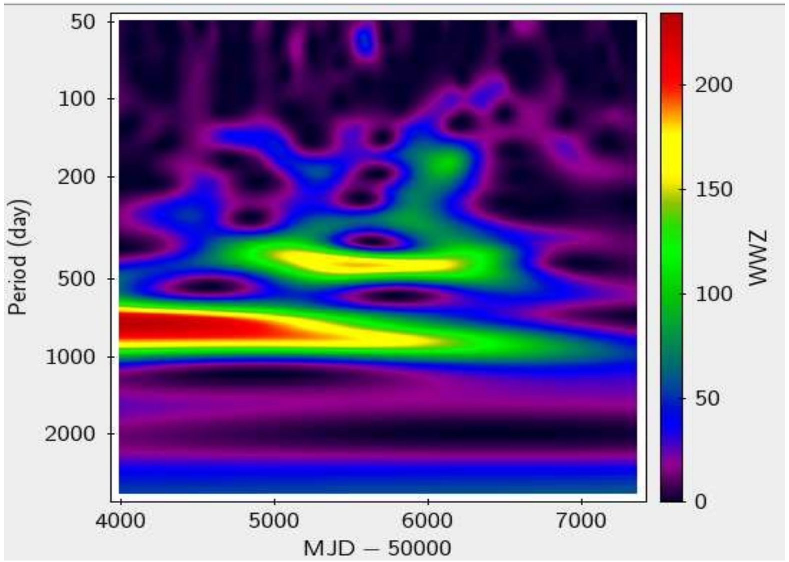

WWZ

270-day radio QPO in the blazar PKS 0219-164

Bhatta, G. 2017, ApJ, 847, 7B

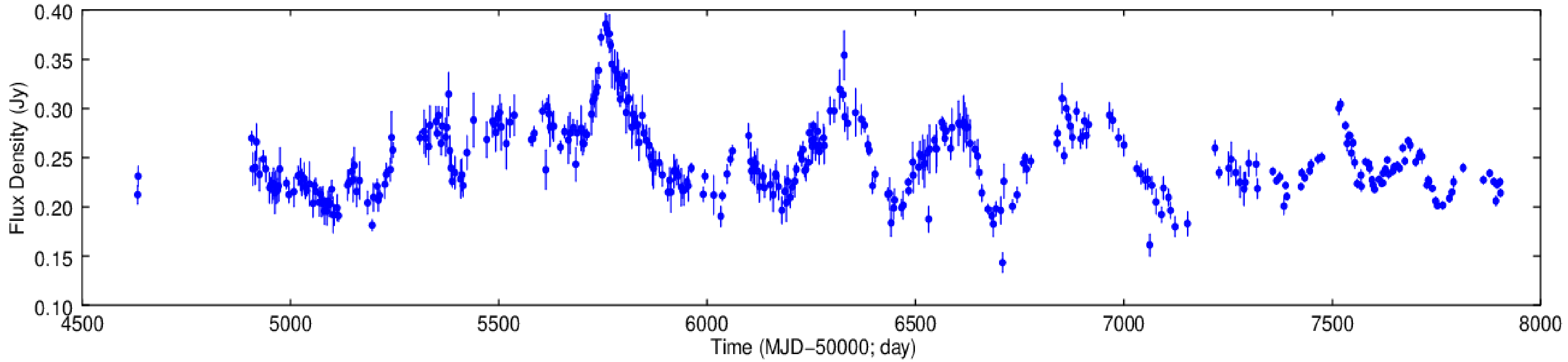

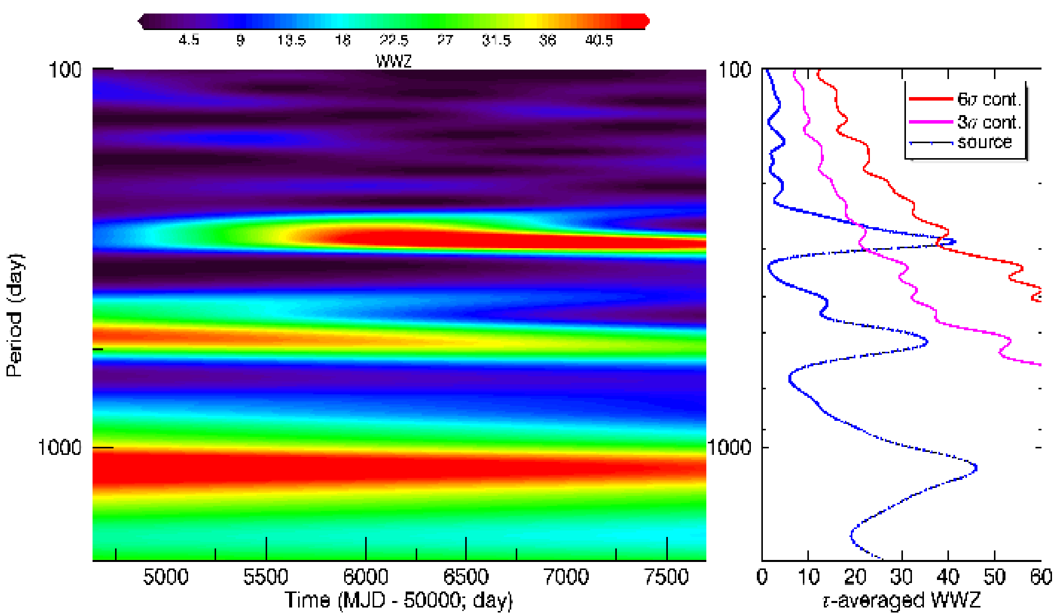

WWZ

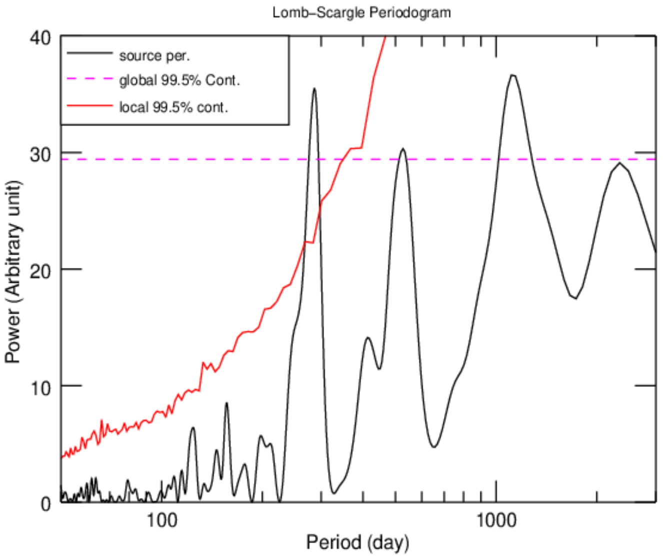

Lomb-Scargle periodogram

560-day Radio QPO in blazar J1043+2408

Bhatta, G. 2018, Galaxy, 6,136B

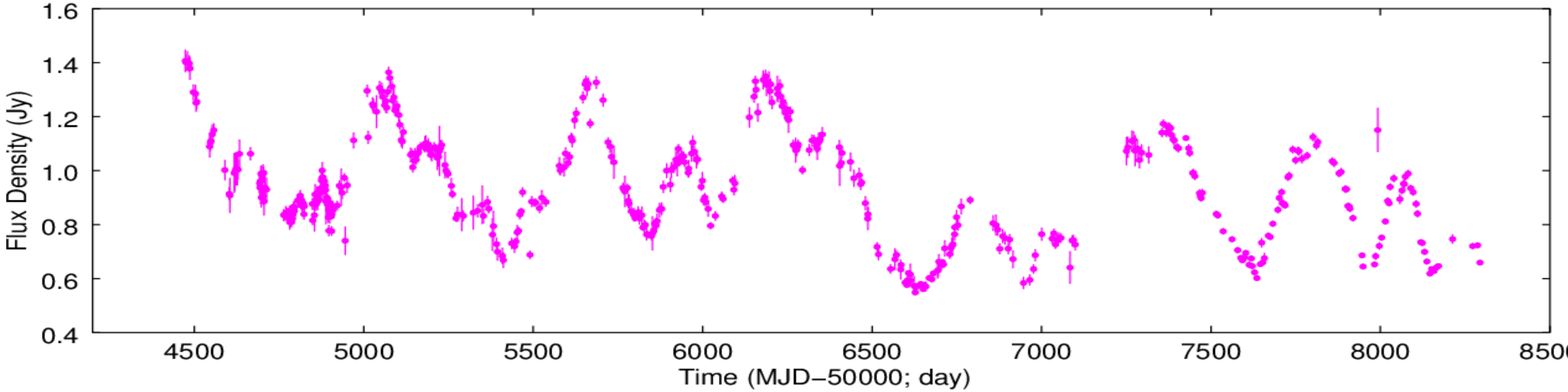

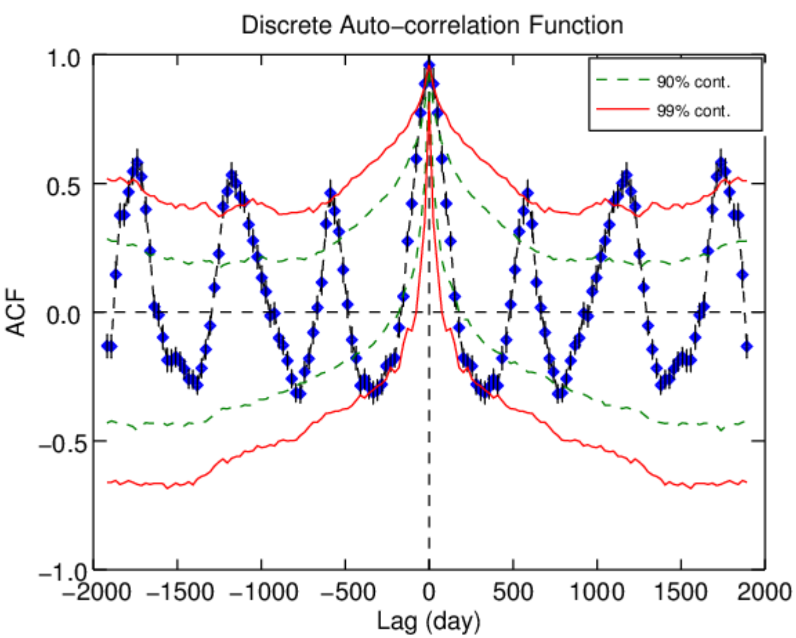

Auto-correlation function

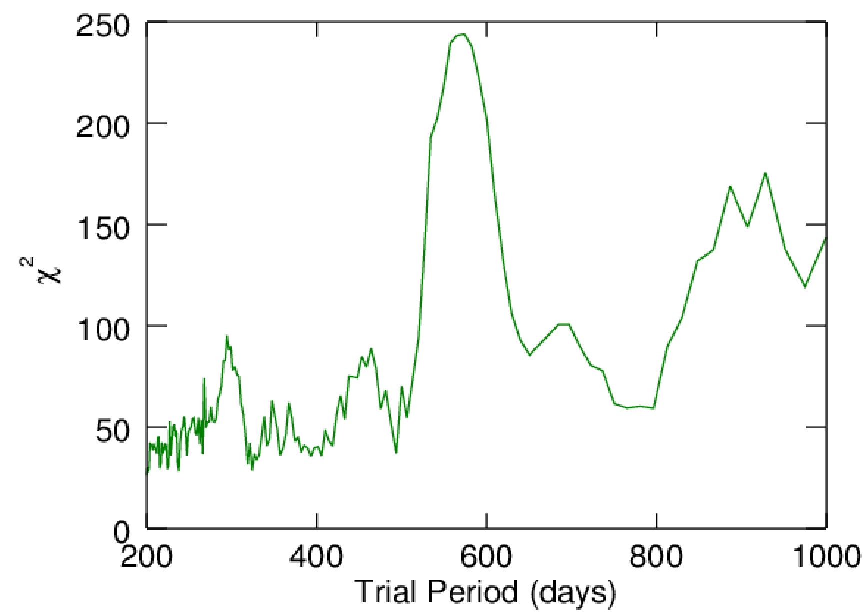

Epoch folding

330 d gamma-ray QPO in Mrk 501

Bhatta, G. 2019, MNRAS

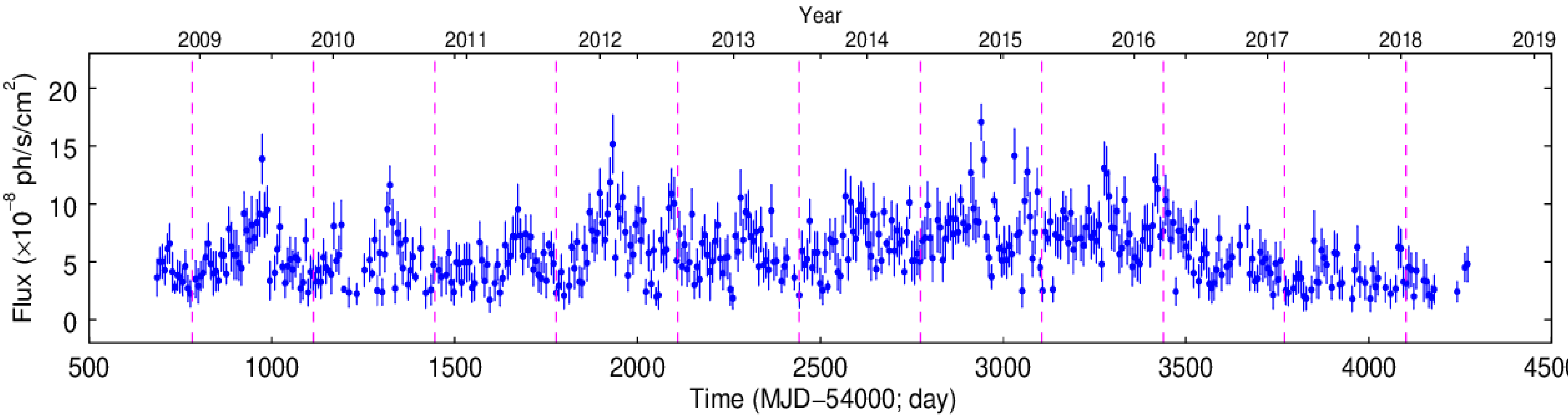

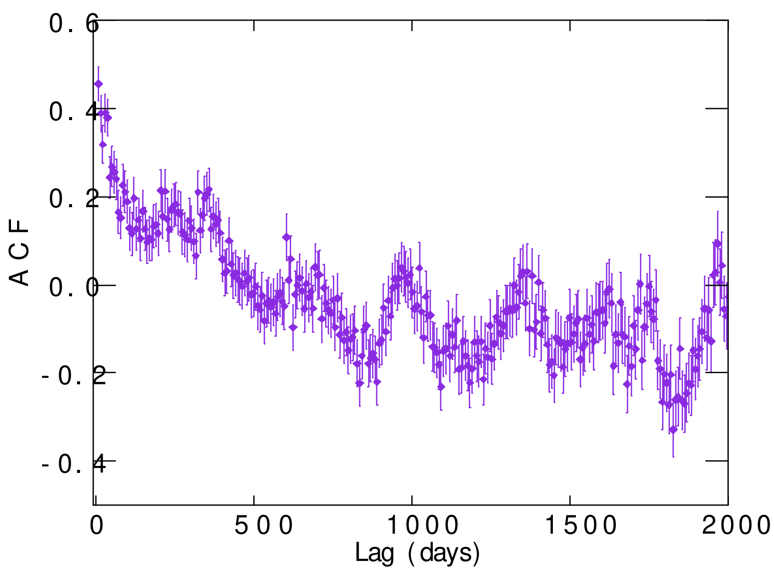

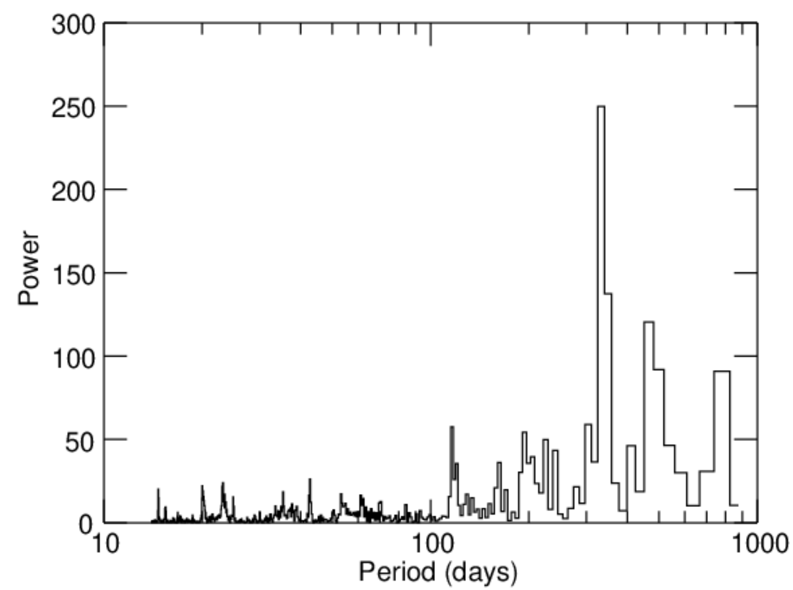

Z-tranformed auto-correlation function

Discrete Fourier transform of ACF

Gamma-ray QPOs in blazars

Study of decade-long light curves of the 20 gamma-ray bright blazars in the energy band of 100 MeV-300 Gev

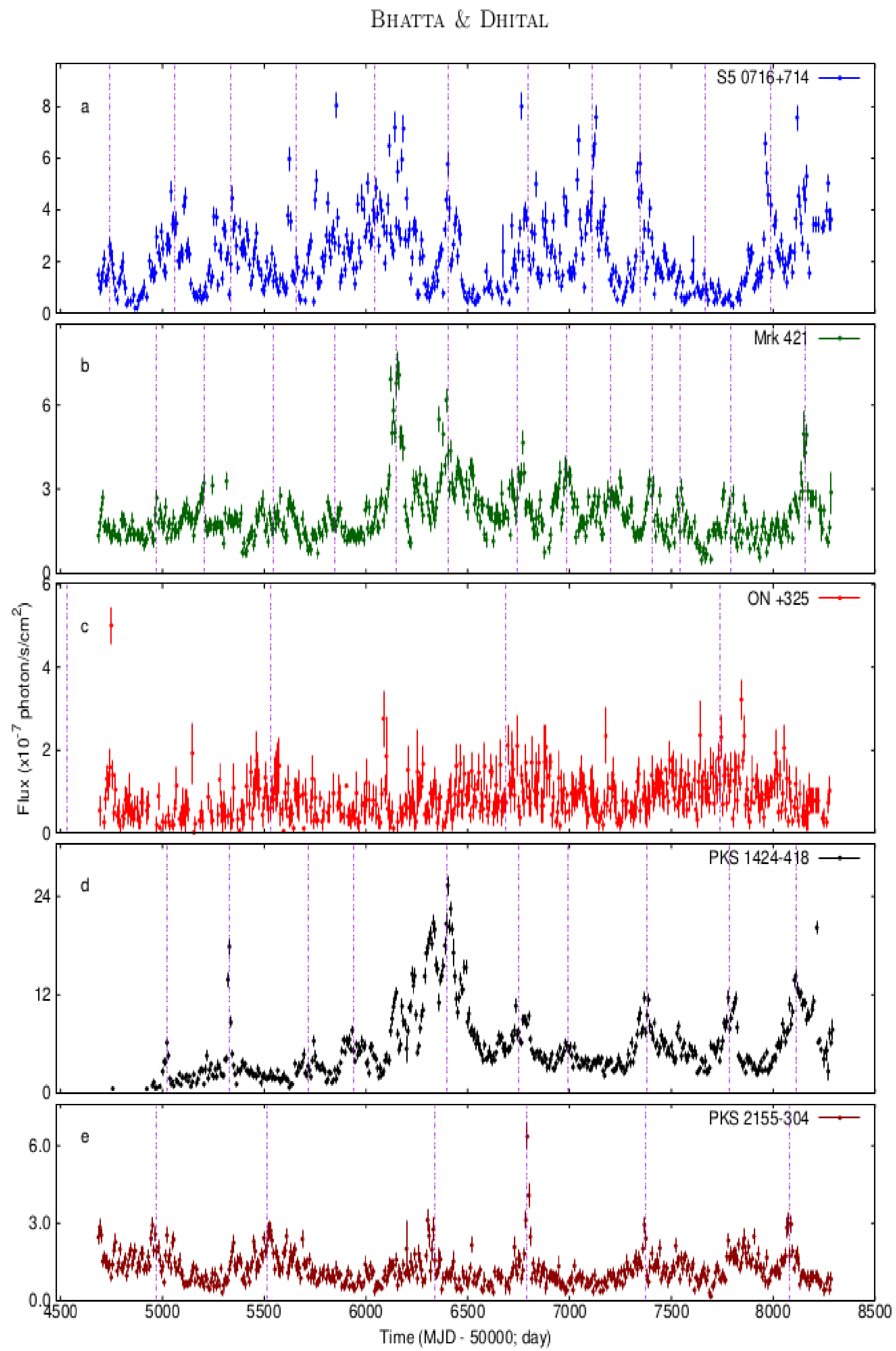

Bhatta, & Dhital 2020, ApJ, 891, 120

Gamma-ray QPOs in blazars

List of the Blazars in the Sample That Show Significant QPO in the γ-Ray Light Curves

	LSP			WWZ		
Source (1)	Period (days) (2)	Local Sig. (%) (3)	Global Sig. (%) (4)	Period (days) (5)	Local Sig. (%) (6)	Global Sig. (%) (7)
S5 716+714	346 ± 23	99.97	99.96	349 ± 27	99.982	99.980
Mrk 421	285 ± 27	99.99	99.97	287 ± 32	99.997	99.993
PKS 2155−304	610 ± 51	99.9994	99.99841	617 ± 53	99.995	99.9981
PKS 1424−418	353 ± 21	99.98	99.95	349 ± 24	99.985	99.981
ON +325	1086 ± 63	99.9986	99.9968	1081 ± 67	99.987	99.983

Bhatta & Dhital 2020, ApJ

Possible explanations

- Binary black hole
- Accretion disk hot spots in Keplerian orbit
- Jet precession, Lense-Thirring precession
- Magnetically arrested disk (MAD) instability
- Emission region moving along helical magnetic field of the jets

Supermassive binary black hole system

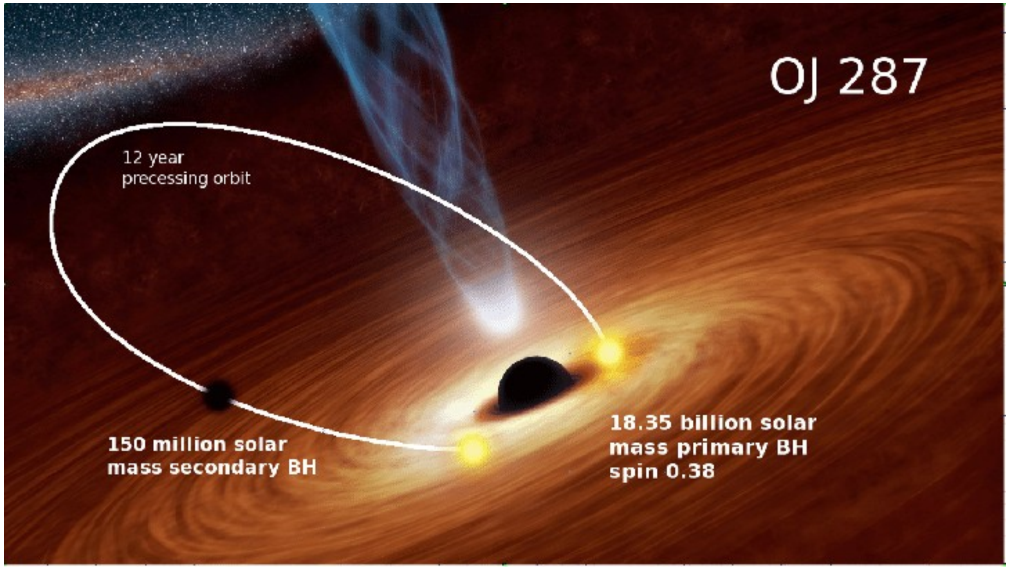

12 year periodicity in OJ 287

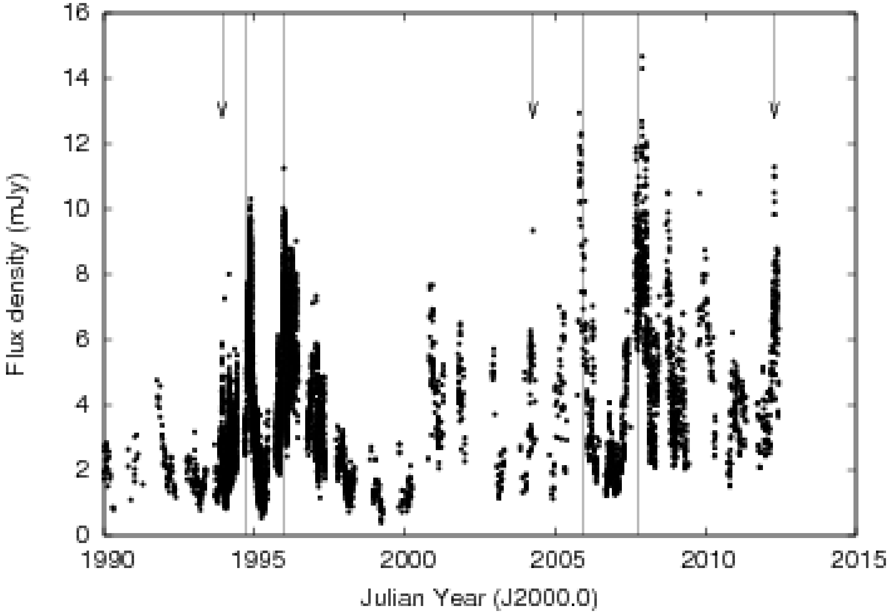

Keplerian period for mass ratio=0.1

$$\tau_k = 0.36 \left(\frac{M}{10^9 M_\odot} \right)^{-1/2} \left(\frac{a}{r_g} \right)^{3/2} \text{days},$$

Disk-jet connection: Relativistic beaming

The periodic oscillations might have their origins in the accretion disk, e.g. revolving hotspots, but the modulations propagate along the jet where they are altered by Doppler beaming

$$F_\nu(\nu) = \delta(t)^{3+\alpha} F'_{\nu'}(\nu)$$

$$\Delta log F = -(3+\alpha)\,\delta\Gamma\beta sin\theta\Delta\theta,$$

$$\delta(t) = 1/\Gamma\,(1-\beta cos\theta(t))$$

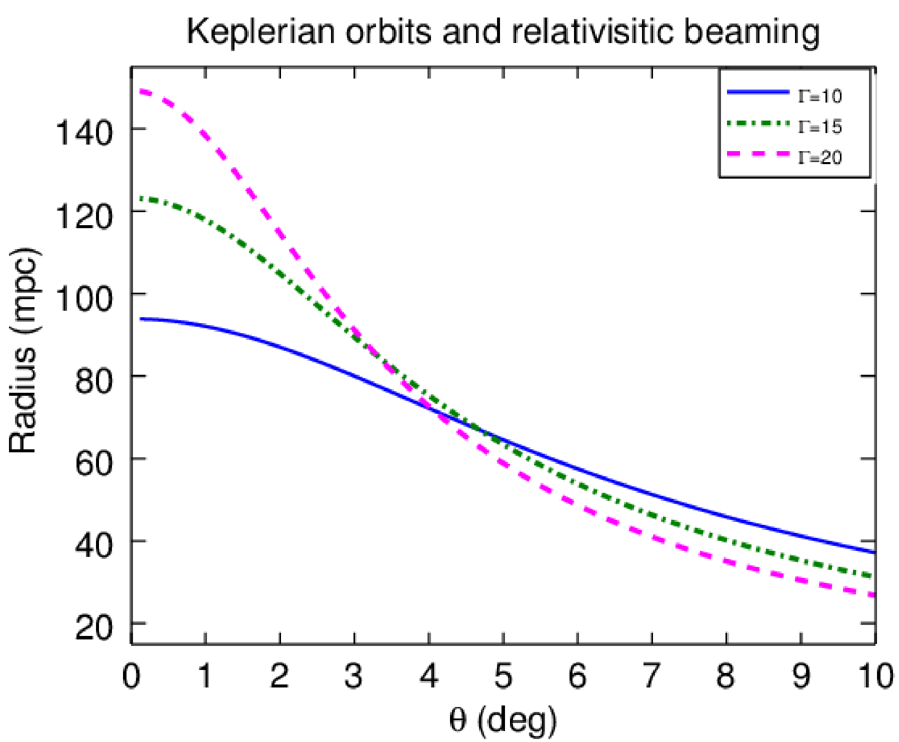

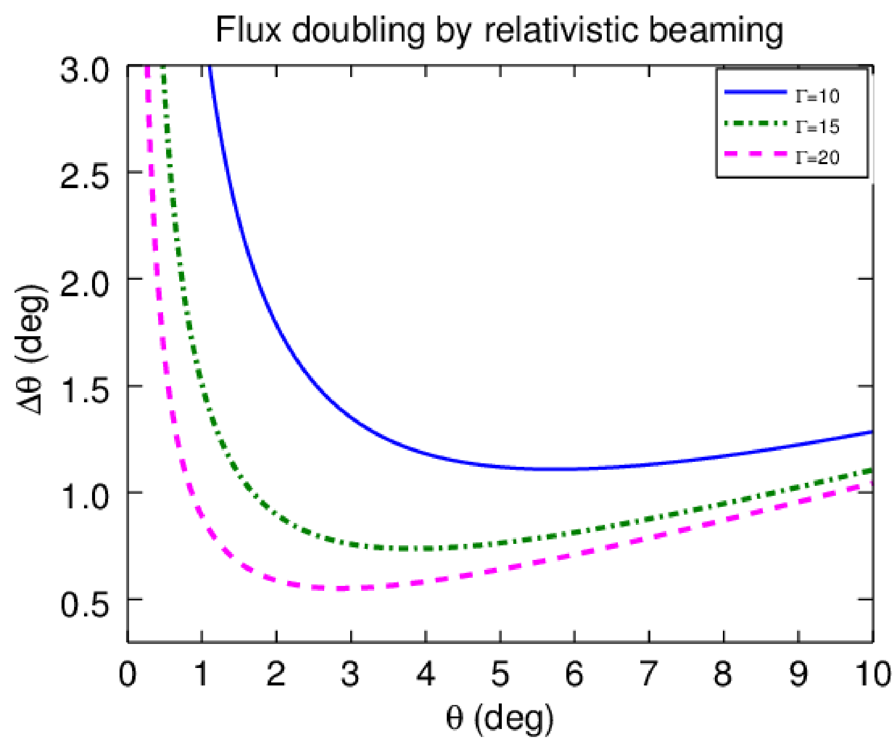

Bhatta, G. 2018, Galaxy, 6,136B

Jet precession

Jet precession due to gravitational perturbation in SMBBH system

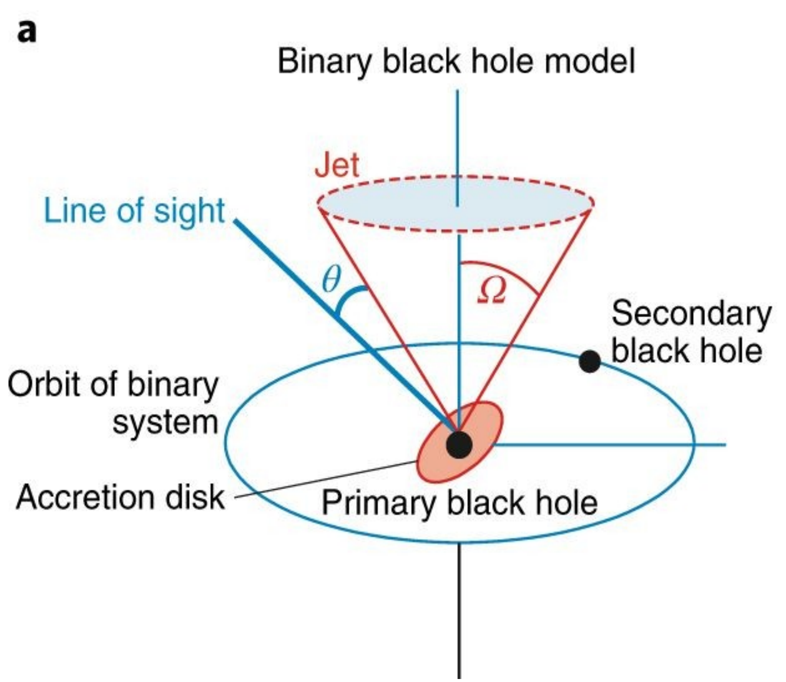

$$P_{\text{prec,s}} = \frac{P_{\text{prec,obs}}}{(1+z)(1-\beta\cos\varphi_0\cos\phi_0)}$$

In misaligned black hole and disk spin, the inner part of the disk undergoes Lense-Thirring precession

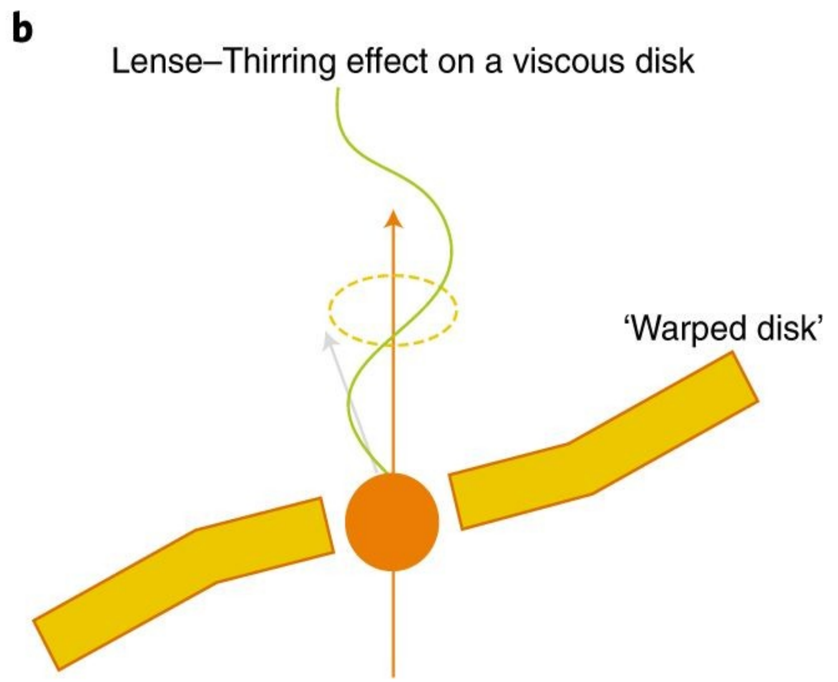

Abraham, Z. 2018, 2018 NatAs, 2, 443A

$$\tau_{LT} = 0.18\left(\frac{1}{a_s}\right)\left(\frac{M}{10^9 M_\odot}\right)\left(\frac{r}{r_g}\right)^3 \text{days}$$

MHD simulations: Magnetically arrested disks (MAD)

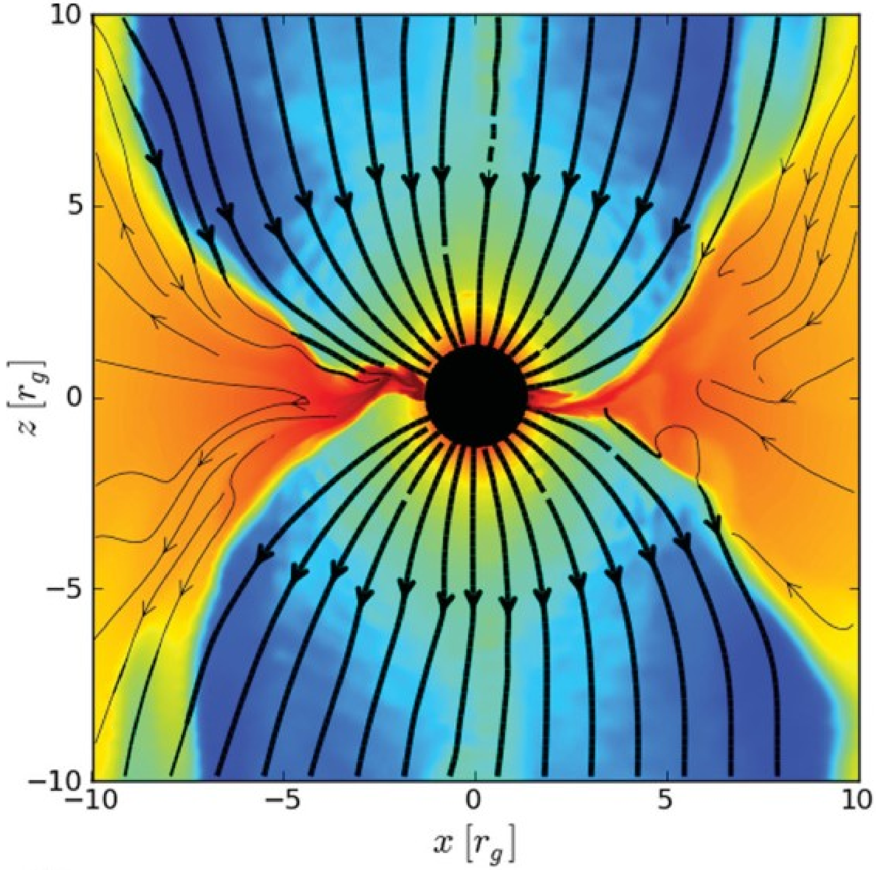

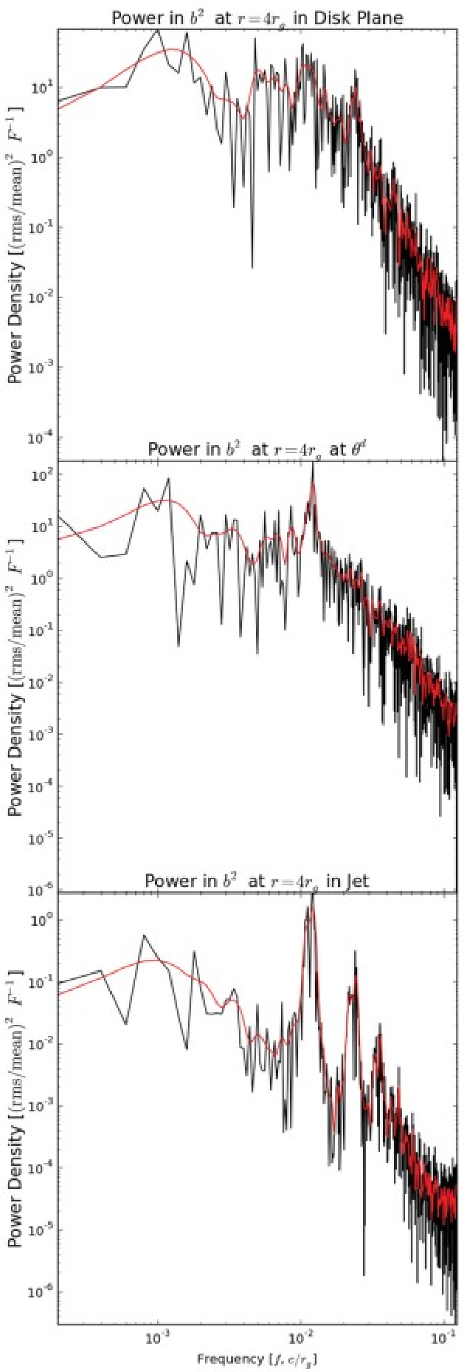

Periodic modulations are set by the BH spin frequency due to the black hole frame dragging the field at the jet-disk interface

McKinney et. al. 2012

Motion along Helical magnetic fields of the jets

Emission regions moving along helical magnetic field show periodicity

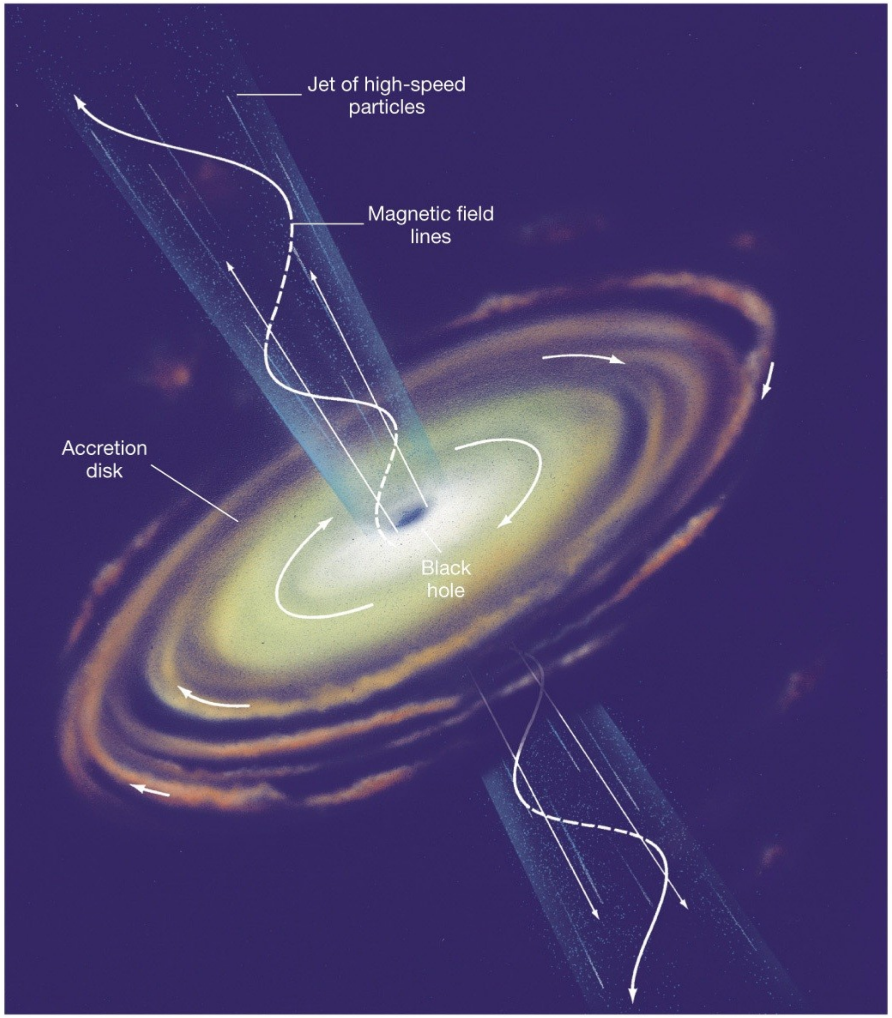

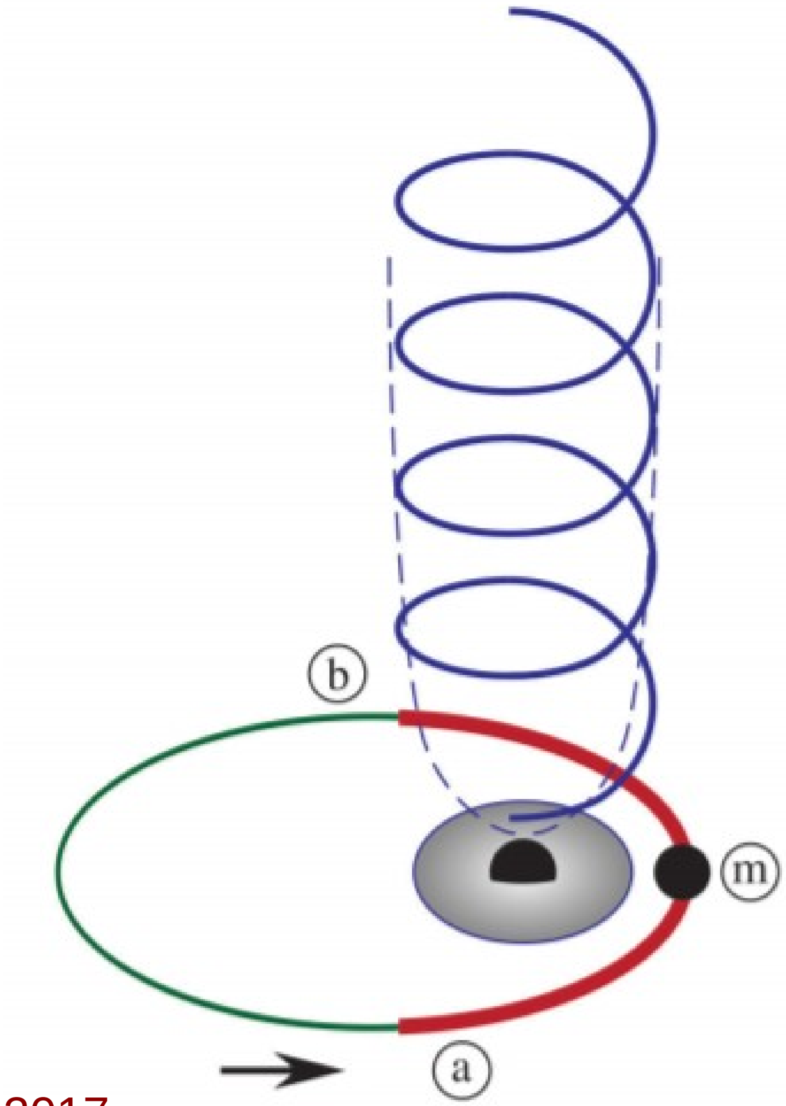

Tavani et al. 2017

Summary and Conclusions

- Several year-scale QPOs seem to be present in the multi-frequency blazar light curves.
- However, finding QPOs in blazars is a challenging task due to several artifacts present is the observation.
- Many models can explain the periodic oscillations
- Multi-frequency approach should break the degeneracy in the models
- Such QPOs could make an excellent probe to the innermost regions of AGN including the extreme physical conditions near the supermassive black hole.

Future direction: Correlation between gamma ray and cosmic rays

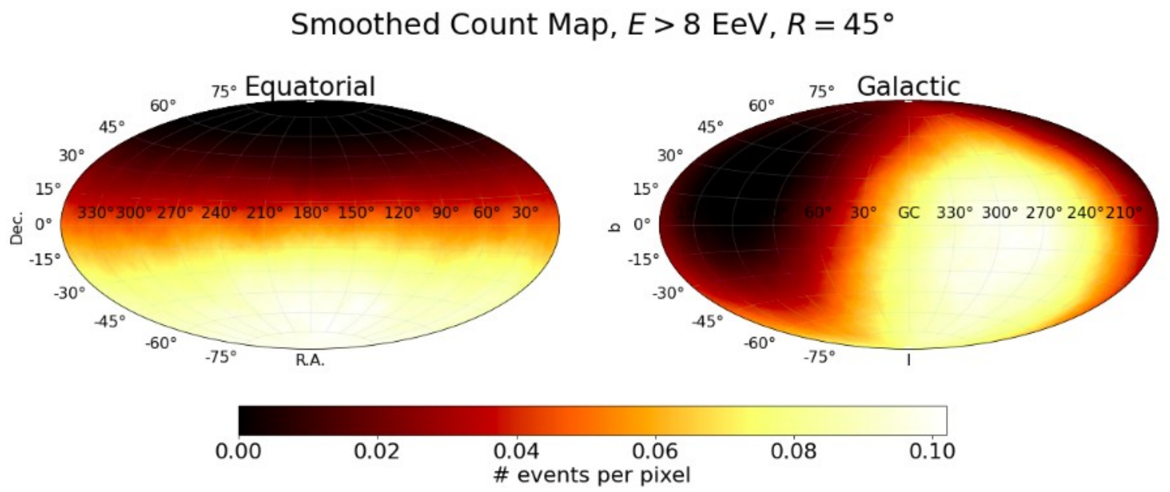

Pierre Auger

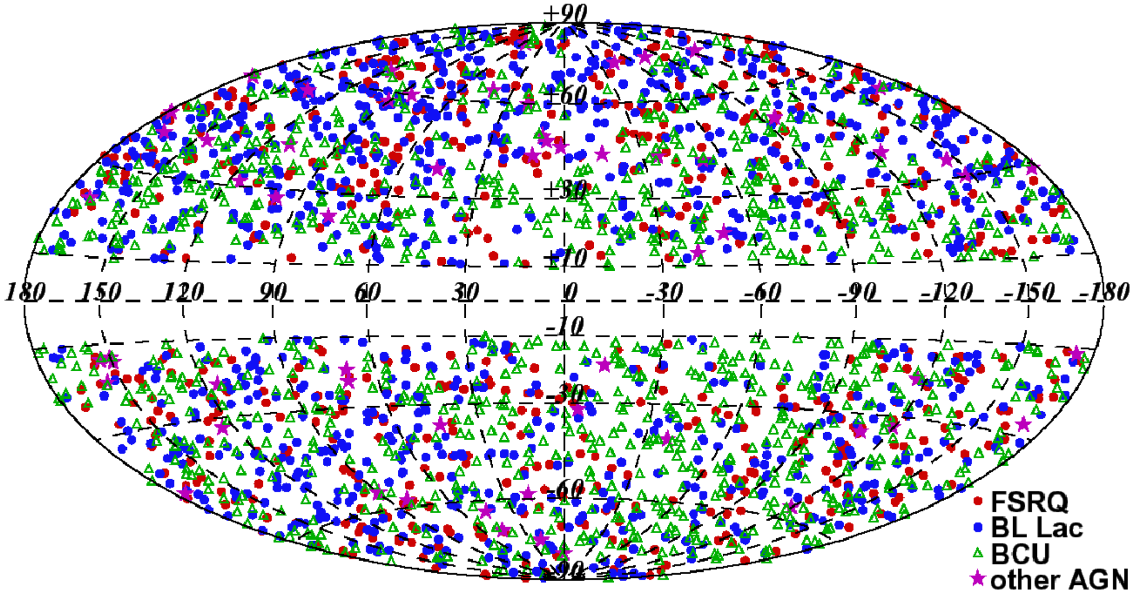

Fermi/LAT 4th Catalog